Context-dependent deposition and regulation of mRNAs in P-bodies

Congwei Wang[1], Fabian Schmich[2,3], Julie Weidner[1], Niko Beerenwinkel[2,3] and Anne Spang[1]
[1]Growth & Development, Biozentrum, University of Basel, Klingelbergstrasse 70, CH-4056 Basel, Switzerland
[2]Department of Biosystems Science and Engineering, ETH Zürich, Mattenstrasse 26, CH-4058 Basel, Switzerland
[3]SIB, Swiss Institute of Bioinformatics, Mattenstrasse 26, CH-4058 Basel, Switzerland

Address of correspondence:
Anne Spang
Biozentrum
University of Basel
Klingelbergstrasse 70
4056 Basel
Switzerland
Phone: + 41 61 267 2380
FAX: + 41 61 267 0759
email: anne.spang@unibas.ch

Abstract

Cells respond to stress by remodeling their transcriptome through transcription and degradation. Xrn1p-dependent degradation in P-bodies is the most prevalent pathway. Yet, P-bodies may facilitate not only decay but also act as storage compartment. However, which and how mRNAs are selected into different degradation pathways and what determines the fate of any given mRNA in P-bodies remain largely unknown. We devised a new method to identify both common and stress-specific mRNA subsets associated with P-bodies. mRNAs targeted for degradation to P-bodies, decayed with different kinetics. Moreover, the localization of a specific set of mRNAs to P-bodies under glucose deprivation was obligatory to prevent decay. Depending on its client mRNA, the RNA binding protein Puf5p either promoted or inhibited decay. The Puf5p-dependent storage of a subset of mRNAs in P-bodies under glucose starvation may be beneficial with respect to chronological lifespan.

Introduction

Cells are often subjected to environmental fluctuations, such as nutrient deficiency, osmotic shock and temperature change. Therefore, cells have evolved a variety of cellular mechanisms to adapt and survive under those conditions, which are generally referred to as stress responses (Mager and Ferreira, 1993). Regulation of transport, translation and stability of mRNAs are among the first acute responses contributing to the rapid adjustment of the proteome. In response to stress, protein synthesis is globally attenuated, but a subset of mRNAs, necessary to cope with the stress, is still subject to efficient translation (Ashe et al., 2000). Non-translating mRNAs are mostly deposited into processing bodies (P-bodies) and stress granules (SGs), which are two types of ribonucleoprotein particles (RNP), conserved from yeast to mammals. As the formation of both granules is induced under diverse stress conditions and a number of components appears to be shared, their precise role in stress response is still a matter of debate (Kulkarni et al., 2010; Mitchell et al., 2013). While P-bodies and SGs both participate in repression of translation and mRNA storage, P-bodies represent also a main site for mRNA degradation through the 5'-decapping-dependent pathway, the 5'-3' exonuclease Xrn1p and transport (Decker and Parker, 2012) (Davidson et al., 2016). In addition to the decay in P-bodies, a 3'-5' exonucleolytic pathway exists (Anderson and Parker, 1998). More recently a co-translational RNA decay pathway has been discovered, which responds to ribosome transit rates (Pelechano et al., 2015; Sweet et al., 2012). Interestingly, some of the P-body components such as the helicase Dhh1p and the exonuclease Xrn1p also act in the co-translational pathway. Moreover, other P-body components such as the decapping activator Dcp2p have been found to associate with polysomes (Weidner et al., 2014). How and which mRNAs are selected into the different pathways, in particular under stress, remains elusive, partly because unbiased methods to identify RNA species are still not widely used. Here, we devised a novel method to identify RNA species in ribonucleotide particles (RNPs), in particular P-bodies.

The protein composition of P-bodies has been extensively studied in both yeast and metazoan (Kulkarni et al., 2010), yet, numerous auxiliary and transient components are still being discovered (Hey et al., 2012; Ling et al., 2014; Weidner et al., 2014), suggesting a tight regulation of the RNA inventory and fate. However, very little is known about the regulation of mRNA fate in P-bodies. To date, the RNA inventory in P-bodies under particular stress remains unclear, and in yeast only a handful of mRNAs have been confirmed to localize to P-bodies (Brengues et al., 2005; Cai and Futcher, 2013; Lavut and Raveh, 2012). Several studies have proposed P-bodies to act not only as decay compartments but also to store and later release RNAs back into the translation pool, particularly upon stress removal. This notion is primarily supported by an observed dynamic equilibrium of mRNA localization between polysomes and P-bodies (Brengues et al., 2005; Kedersha et al., 2005; Teixeira et al., 2005). Recently this model has been challenged and it was proposed that Xrn1p-dependent decay might occur outside P-bodies (Sweet et al., 2012), which is supported by findings that the 5' decapping machinery is present at membrane-associated polysomes under non stress conditions (Huch et al., 2016; Weidner et al., 2014). Still, a prevailing hypothesis in the field is that specific mRNAs preferentially accumulate in P-bodies under different stresses promoting cell adaption and survival (Decker and Parker, 2012). In support of this concept, the number, morphology and half-life of P-bodies vary depending on the particular stress. For example, under glucose starvation only a few, large, long-lived P-bodies are observed, whereas Ca^{2+} stress produces numerous, small P-bodies that disappear within 30 to 45 min after the initial induction (Kilchert et al., 2010). Lacking a global picture of mRNA species in P-bodies greatly hinders the study of the functional role of P-bodies in mRNA turnover and stress response.

A major obstacle in the universal identification of mRNAs present in P-bodies is that at least a portion of the transcripts are likely engaged in deadenylation or degradation, and, hence, commonly used oligo(dT) purification provides an incomplete and biased picture of mRNAs present in P-bodies. We overcame this obstacle by adapting and improving a crosslinking affinity

purification protocol (Weidner et al., 2014) to globally isolate P-body associated transcripts. We demonstrate that P-bodies contain distinct mRNA species in response to specific stresses. The sequestered transcripts underwent different fates depending on their function, for example: mRNAs involved in overcoming stress were stabilized while others were degraded. Similarly, mRNA decay kinetics differed depending on the mRNA examined. Our observations are consistent with a dual role of P-bodies in mRNA degradation and storage. Under glucose starvation, the RNA-binding protein Puf5p plays a central role as it regulates the decay of a set of mRNAs and is also responsible for the localization and stability of another set. Moreover, the stabilization of at least one mRNA in a Puf5-dependent manner may contribute to chronological lifespan.

Results

A novel method to isolate RNAs sequestered into P-bodies

To determine the mRNA species sequestered into P-bodies upon different stress conditions, we combined and improved a method based on *in vivo* chemical crosslinking and affinity purification, which we had previously used to identify regulators and protein components of P-bodies (Weidner et al., 2014) with commonly used techniques to generate RNA libraries for subsequent RNA-Seq (Hafner et al., 2010; Kishore et al., 2011) (Figure 1A). We refer to this method as chemical Cross-Linking coupled to Affinity Purification (cCLAP). We have shown earlier that P-bodies in yeast are in very close proximity to the endoplasmic reticulum (ER) and that they fractionate with ER membranes (Kilchert et al., 2010; Weidner et al., 2014). To explore the mRNA content of P-bodies, either Dcp2p or Scd6p, which are part of the 5' and the 3'UTR-associated complex of P-bodies, respectively, were chromosomally tagged with a His_6-biotinylation sequence-His_6 tandem tag (HBH) (Tagwerker et al., 2006; Weidner et al., 2014). P-bodies were either induced through glucose starvation or through the addition of $CaCl_2$ or NaCl. We chose $CaCl_2$ as stressor because secretory pathway mutants induce P-bodies through a Ca^{2+}/calmodulin-dependent pathway, which is mimicked by the addition of Ca^{2+} to the medium (Kilchert et al., 2010). Notably, this induction pathway is different from the one employed by the cell upon glucose starvation. NaCl was selected as an alternative hyperosmotic stress to determine whether different hyperosmotic stresses would elicit the same or different responses. We chose formaldehyde as cross-linking agent because it can be directly applied to the culture medium and is easily and rapidly quenchable allowing precise cross-linking conditions without introducing any unwanted stress like through centrifugation or medium changes prior to the cross-link reaction. Yeast cells were exposed to stress for 10 min, cross-linked and, after lysis, P-bodies were purified from the membrane fraction through the HBH-tag present on either Dcp2p or Scd6p. We chose to stress the cells for only 10 min in order to exclude any contribution of SG, which are not present at this

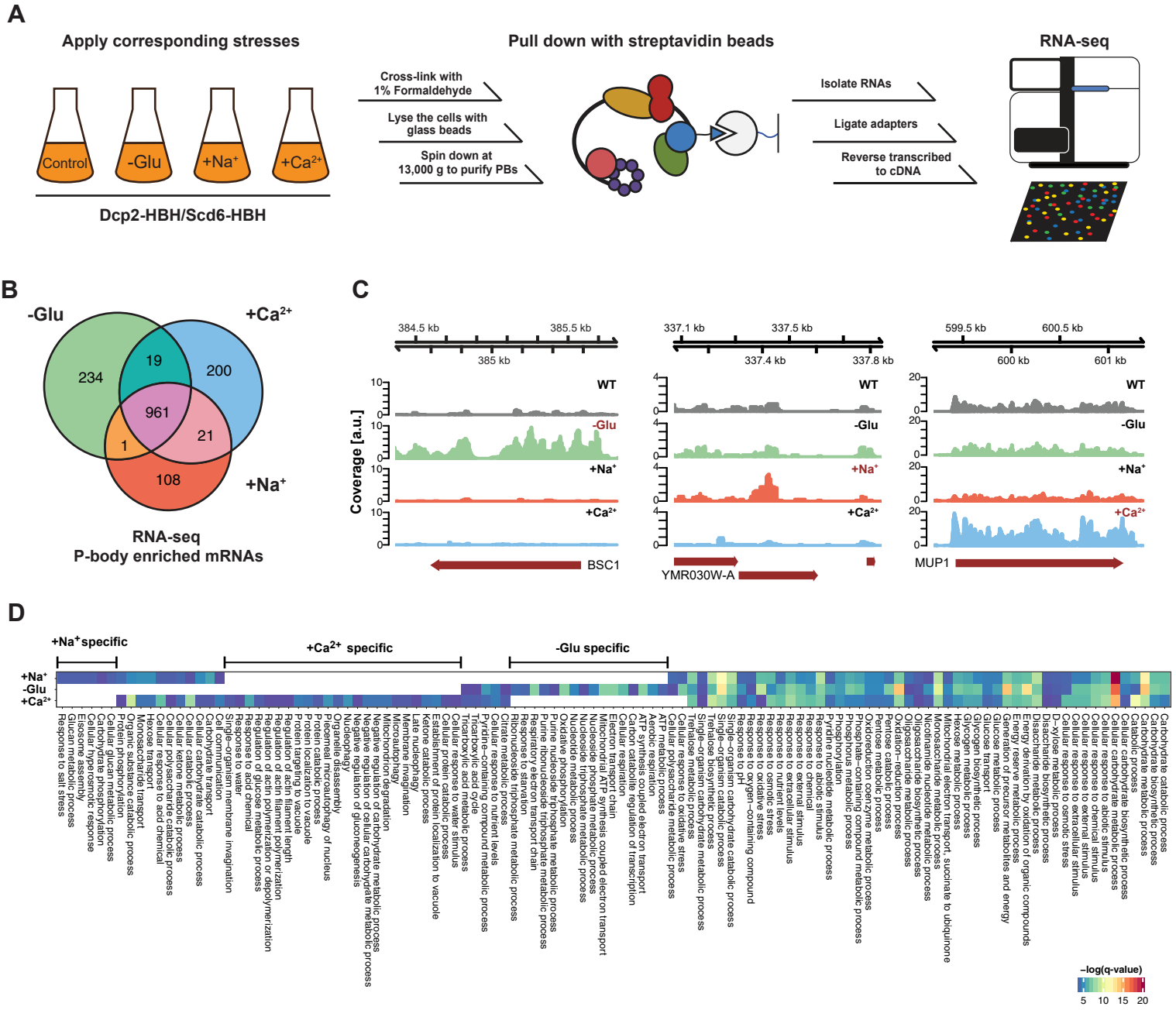

Figure 1. RNA-Seq reveals stress-specific mRNA subsets enriched in P-bodies.
(A) RNA-Seq library preparation workflow. Cells expressing Dcp2-HBH or Scd6-HBH were stressed for 10 min, followed by cross-linking with formaldehyde. After cell lysis, centrifugation was performed to enrich membrane fractions. Cross-linked complexes were subsequently purified via streptavidin affinity purification. mRNAs were isolated and ligated with adapters. cDNA libraries were prepared by reverse transcription and sequenced using single-read RNA-Seq. (B) Venn diagram illustrating the intersections among mRNAs enriched in P-bodies (p<0.05) under glucose depletion and osmotic stress conditions with Na^+ or Ca^{2+}, relative to the no stress condition as determined by RNA-Seq. (C) Read coverage plots (average over five biological replicates) of RNA-Seq data mapped to P-body enriched genes under specific stress conditions. (D) Enrichment analysis of P-body associated genes under different stress conditions against Gene Ontology's (GO) biological processes (BP). Significantly enriched pathways (q-value <0.05) from hypergeometric tests are presented in a clustered heatmap. Rows and columns correspond to stress conditions and pathways, respectively, and the negative logarithms of q-values are color-coded from blue (low) to red (high).

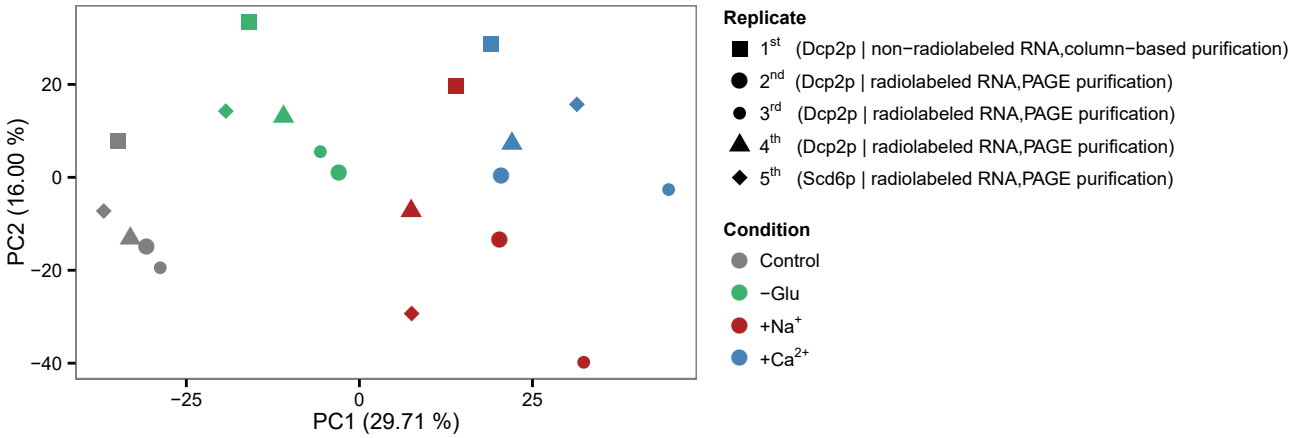

Figure 1- Figure Supplement 1. Reproducibility of datasets derived from RNA-Seq.
Principal component analysis (PCA) plot based on the read count profile from aligned RNA-Seq data of five biological replicates for each condition. The two first principal components are plotted with the proportion of variance explained, indicated by each component next to the axes labels.

time point (Kilchert et al., 2010). Libraries for RNA-Seq were prepared in two ways: either using PAGE purification with radiolabeled mRNAs or using a column-based purification method (Table S1).

Principal Component Analysis (PCA) performed on the read count profile for each condition from the aligned RNA-Seq data of the five independent biological replicates generated four clusters, corresponding perfectly to the three stress conditions plus the unstressed control (Figure 1- Figure Supplement 1). Neither the tagged P-body component nor the purification method used for RNA-Seq sample preparation perturbs the clustering pattern, indicating a high degree of reproducibility of our method. Given that we used two types of hyperosmotic stress, it is not surprising that the Ca^{2+} and Na^{+} datasets cluster more closely than the ones derived from glucose starvation conditions. Yet, being able to detect differences between the two osmotic shock conditions further exemplifies the robustness of our approach. Therefore, cCLAP is a valid method to determine the RNA content of RNPs.

The nature of P-body sequestered RNAs is stress-dependent

In total, we identified 1544 mRNAs statistically significantly enriched in P-bodies under glucose depletion and Na^{+} and Ca^{2+} stresses, relative to the unstressed condition (Figure 1B and Table S2). While about 65% of the detected mRNAs were common between stresses, approximately 35% of the RNAs were specific to an individual stress (Figure 1B). Reads on stress-specific targets were distributed over the entire length without any preferential accumulation or depletion at the 5' or 3' UTRs as exemplified by the selected transcripts (Figure 1C).

If mRNA deposition in P-bodies was context-dependent, one would expect an enrichment of mRNAs belonging to the same pathways/processes. To test this notion, we employed Gene Ontology (GO) enrichment analysis (biological process) (Figure 1D). Consistent with the Venn diagram (Figure 1B), a number of biological processes were shared by all three stress conditions, yet many GO terms were specific to one particular stress, suggesting that mRNA sequestration in P-bodies is, in general, context-dependent. For example, within the glucose specific set, we

found a group of processes related to mitochondrial oxidative phosphorylation (herein referred to as mitochondria-related mRNAs). This group is of particular interest, as mitochondria respiration genes are generally up-regulated upon glucose starvation (Wu et al., 2004). Taken together, our data suggest that a subset of mRNAs is sequestered in P-bodies in a stress-dependent manner.

mRNAs localize to P-bodies in a context-dependent manner

Thus far, we have shown that mRNAs can be cross-linked to P-body components in a stress-dependent manner. To demonstrate that these mRNAs indeed localize to P-bodies, we employed fluorescence *in situ* hybridization coupled to immunofluorescence (FISH-IF; Figure 2A). We used Dcp2p as P-body marker for immunofluorescence. Since P-bodies exhibit a compact, dense structure (Souquere et al., 2009), the generally employed long probes (up to 1,000 nt) are not suitable for detection of mRNA in P-bodies. However, using multiple 50-100 nt FISH probes (4-8 per transcript) allowed us to detect specific mRNAs in P-bodies, as the no probe control only exhibited background staining (Figure 2, Figure 2- Figure Supplement 1A). Regardless, we may not be able to detect all mRNA molecules and are likely underestimating the extent of localization of mRNAs within P-bodies. Moreover, transcripts in yeast are often present in less than 10 copies per cell (Zenklusen et al., 2008), which may hinder detection by this method. Finally, most mRNAs are degraded in P-bodies (Sheth and Parker, 2003), therefore any given mRNA may be detected in P-bodies at any given time. Taken theses constraints into consideration, we set the threshold at ≥ 1.5 fold enrichment over control mRNAs to determine P-body association.

We selected a set of mRNAs from each stress condition and determined their subcellular localization. Upon glucose depletion, seven mRNAs including both non-mitochondria-related (*BSC1*, *TPI1*, *RLM1*) and mitochondria-related (*ATP11*, *ILM1*, *MRPL38*, *AIM2*) groups, based on the GO pathways, showed significant co-localization with P-bodies (Figure 2B, 2C) relative to background (Figure 2- Figure Supplement 1B, C). To validate that the mRNA localization to P-bodies is stress-specific, we repeated the FISH-IF under osmotic stresses for three mRNAs (Figure 2D). None of them was significantly enriched in P-bodies under these stress conditions

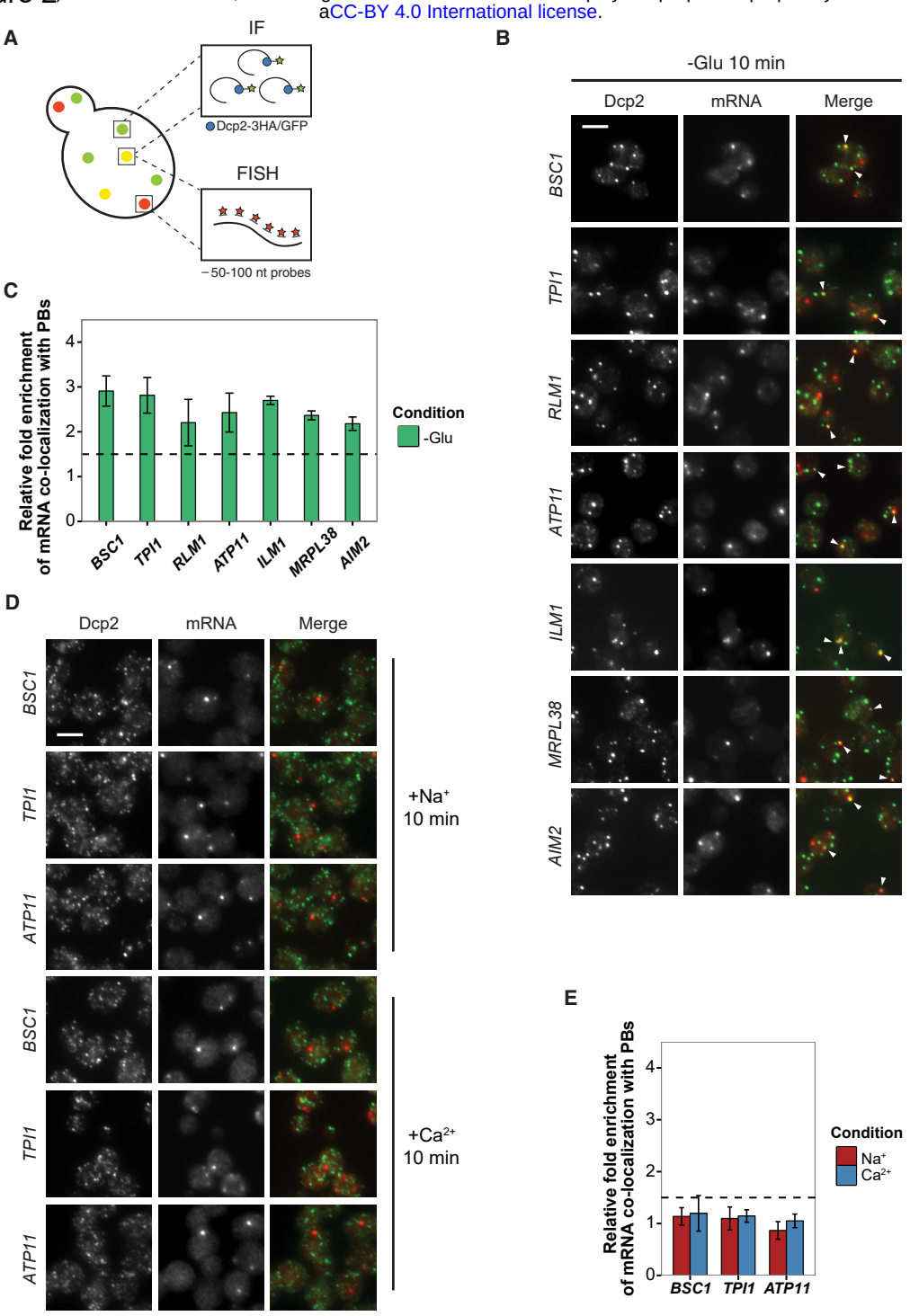

Figure 2. Validation of glucose-specific candidates by combined fluorescence in situ hybridization and immunofluorescence (FISH IF).

(A) Schematic representation of combined FISH-IF technique. Immunofluorescence staining was performed against P-body marker Dcp2 chromosomally tagged with 3HA or GFP. To detect mRNAs accumulating in P-bodies, multiple short probes (50-100 nt) against the open reading frame (ORF) of each gene were used for FISH. (B) Fluorescence images of P-bodies and glucose-starvation-specific candidate mRNAs after glucose depletion. Cells expressing Dcp2-3HA were first grown in YPD media to mid-log phase and shifted to YP media lacking glucose for 10 min. Scale bar, 5 μm. Error bars, Mean ± SEM. (C) Bar plot depicting the quantification of co-localization between candidate mRNAs and P-bodies. The percentage of co-localization was quantified as described in Materials and Methods. The relative fold enrichment was subsequently calculated by normalizing the percentage of candidate mRNAs against the percentage of control mRNAs (Figure 2- Figure Supplement 1C). The dashed line represents an arbitrarily fixed threshold of 1.5 for determining significant P-body association. (D) Fluorescence images of P-bodies and glucose-specific candidate mRNAs under mild osmotic stress with Na^+ or Ca^{2+}. Cells expressing Dcp2-3HA were first grown in YPD media to mid-log phase and shifted to YPD media containing 0.5 M NaCl or 0.2 M $CaCl_2$ for 10 min. Scale bars, 5 μm. Error bars, Mean ± SEM. (E) Same as (C) except stress conditions. Scale bar, 5 μm. Error bars, Mean ± SEM.

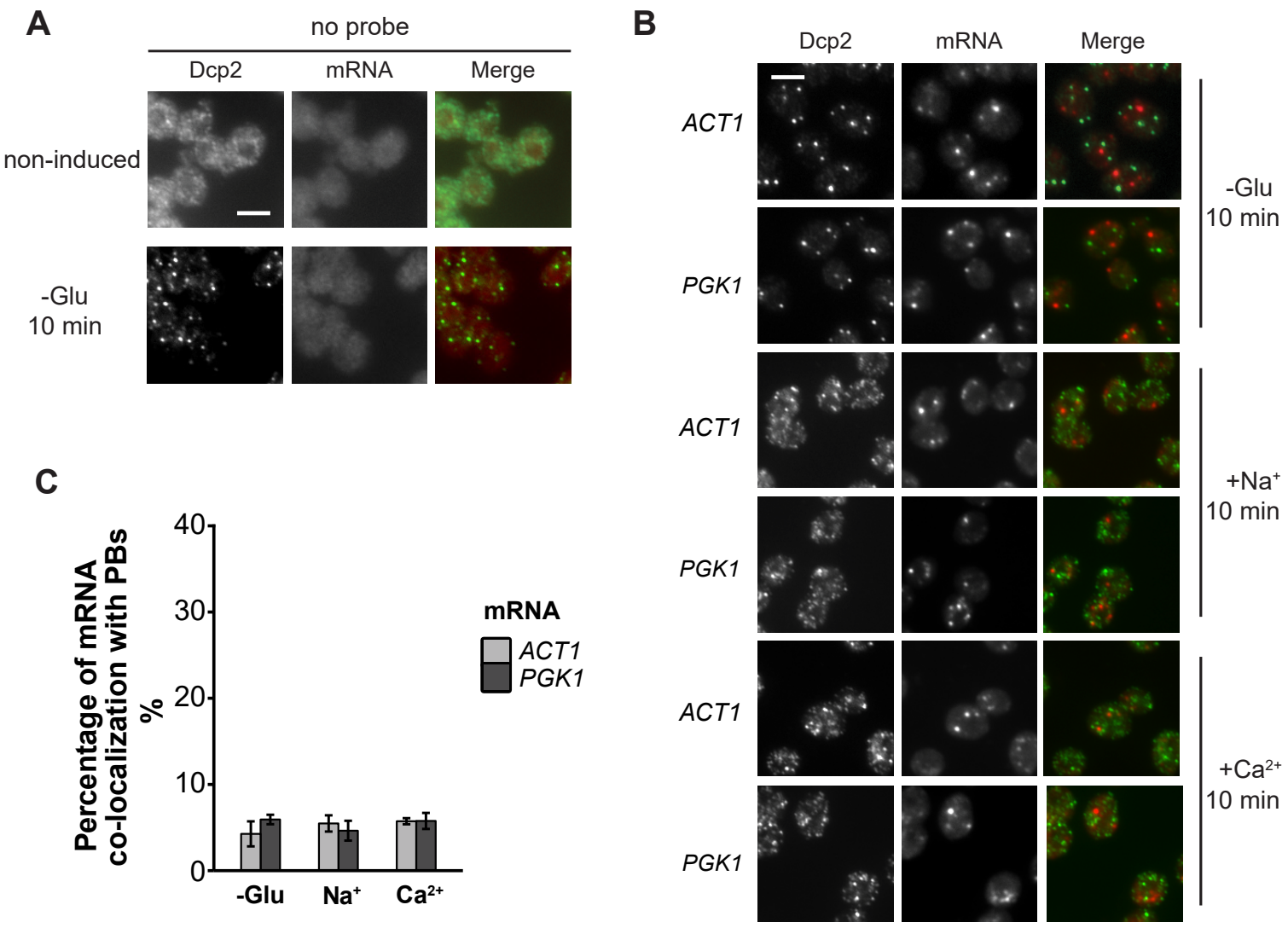

Figure 2- Figure Supplement 1. Evaluation of non-candidate mRNAs by FISH-IF.
(A) FISH-IF controls. Combined FISH-IF was performed without probes with cells expressing Dcp2-3HA under non-induced condition. Scale bar, 5 μm. (B) Fluorescence images of P-bodies and two non-candidate mRNAs, *ACT1* and *PGK1*. Cells expressing Dcp2-3HA were treated with indicated stresses. Scale bar, 5 μm. (C) Bar plot depicting the percentage of co-localization between non-candidate mRNAs and P-bodies. The average of the percentages of *ACT1* and *PGK1* under each condition served as a control level in calculating the fold enrichment in Figure 2C, 2E, 4B, 5C and 4S1D. Error bars, Mean ± SEM. Scale bar, 5 μm.

(Figure 2E). Similarly, we found mRNAs that were specifically enriched in P-bodies under a unique osmotic condition but not under the other stresses (data not shown). We conclude that at least a subset of mRNAs must be selected for -or spared from- transport to P-bodies in a context-dependent manner.

mRNAs experience divergent fates inside P-bodies

It has been proposed that mRNAs are not only decayed in P-bodies, but may be stored there and re-enter translation after stress subsides (Brengues et al., 2005). We found mRNAs that were potentially excellent candidates for being stored in P-bodies. The mitochondria-related genes were transcriptionally up-regulated following glucose starvation (Figure 3- Figure Supplement 1A), while at the same time transcripts were sequestered in P-bodies. To investigate the fate of P-body associated mRNAs further, we employed the 4-TU non-invasive pulse-chase RNA labeling technique followed by qRT-PCR. With this technique, we can specifically label RNA before stress application and determine its decay rate (Munchel et al., 2011) (Figure 3A). To differentiate P-body specific degradation from the exosome decay pathway, we analyzed the mRNA half-life in the presence and absence of the P-body 5'-3' exonuclease Xrn1p (Figure 3B). *ACT1* was used as endogenous reference gene due to its high stability during glucose starvation (Figure 3- Figure Supplement 1B). No significant reduction in mRNA levels was observed for Group II mRNAs (*ATP11*, *ILM1*, *MRPL38* and *AIM2*) for up to one hour of glucose withdrawal, suggesting that those transcripts were stabilized inside P-bodies (Figure 3B, Group II). Consistently, after a rapid initial increase, the total transcript levels remained constant over the time course (Figure 3- Figure Supplement 1A, Group II). Conversely, the transcripts within group I (*BSC1*, *TPI1*, and *RLM1*) underwent Xrn1p-dependent decay (Figure 3B, Group I). Intriguingly, the onset and the kinetic of the decay varied from mRNA to mRNA, indicating that individual intrinsic properties of the mRNAs may determine their half-lives within P-bodies. Likewise, the total mRNA levels were modulated in a similar way (Figure 3- Figure Supplement 1A, Group I), hinting towards coordination between P-body specific decay and transcription. Our data provide strong evidence that the decay kinetics

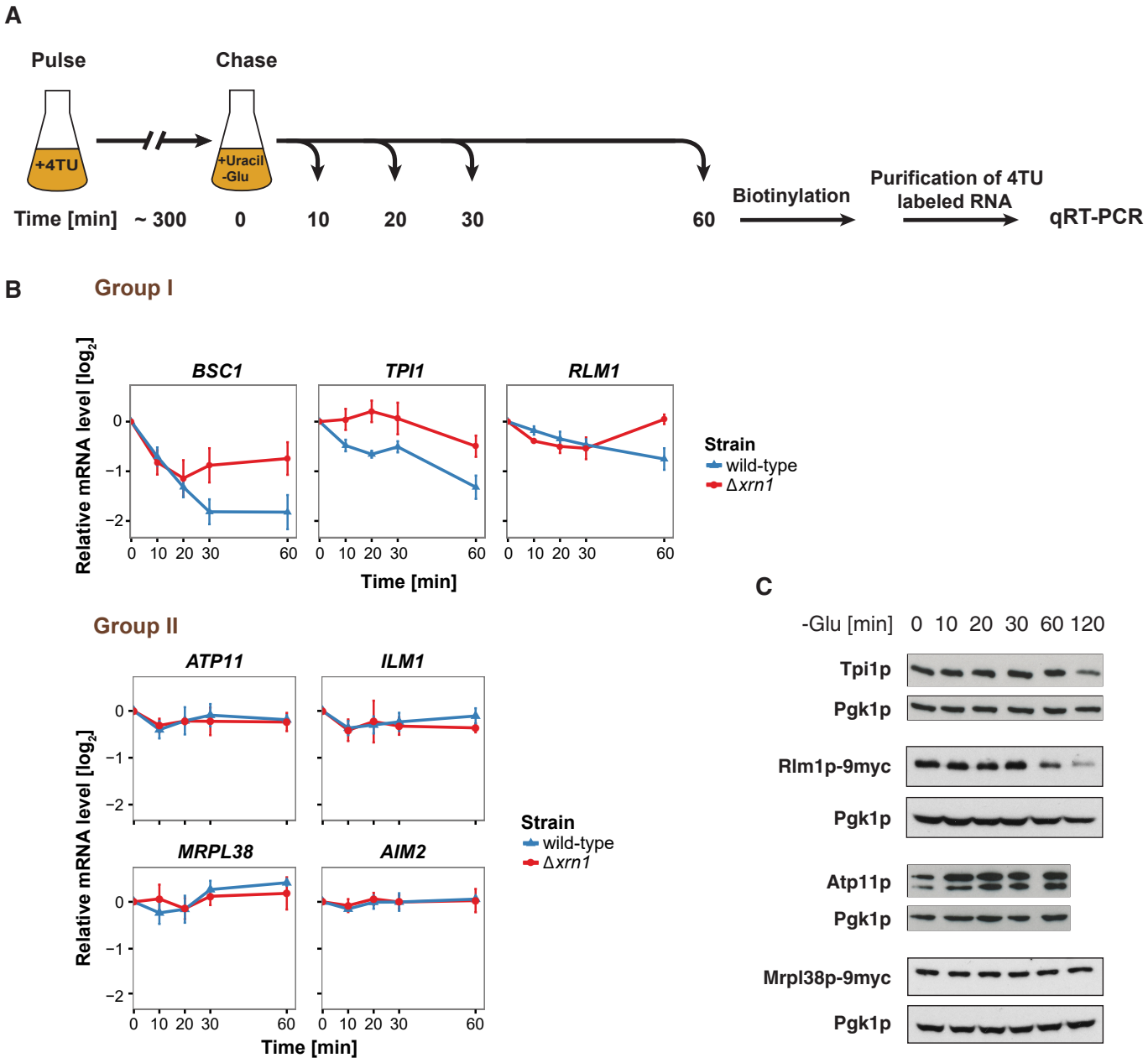

Figure 3. The stability of P-body enriched mRNAs varies and can be categorized according to their GO terms. (A) Schematic illustration of pulse-chase protocol. Cells were grown in the presence of 0.2 mM 4TU and shifted into media lacking glucose but containing 20 mM uracil. Cells were harvested at indicated time points after the shift. Total RNA was extracted and biotinylated. 4TU labeled RNA was purified and subsequently analyzed by qRT-PCR. (B) The stability of 4TU labeled candidate mRNAs was determined by qRT-PCR in wild type and Δ*xrn1* strains at indicated time points following a shift to glucose-depleted media. Transcription levels were normalized using *ACT1* gene as an endogenous reference. Group I: non-mitochondria-related candidates. Group II: mitochondria-related candidates. Error bars, Mean ± SEM. (C) Western blot analysis of Tpi1p, Rlm1p-9myc, Atp11p and Mprl38p-9myc at indicated time points after glucose deprivation. The 9myc tag was inserted at the end of the coding sequence without affecting the 3'UTR. Pgk1p was used as a loading control. Anti-Tpi1p, anti-Atp11p, anti-myc and anti-Pgk1p were used for detection. Results are representative of 3-4 independent experiments per target protein.

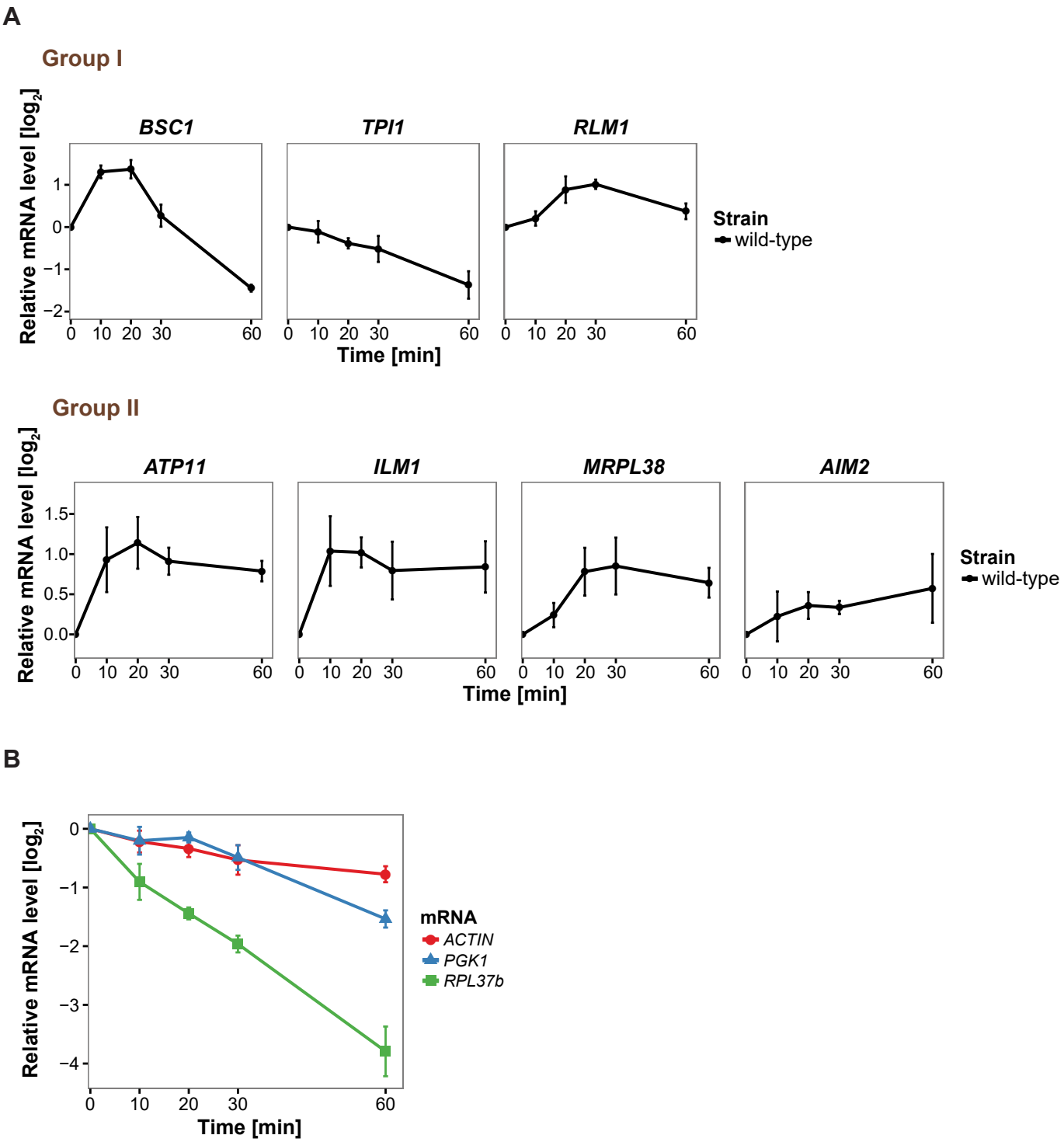

Figure 3- Figure Supplement 1. Changes in total candidate mRNA levels corresponding to Xrn1-dependent degradation.

(A) Evaluation of qRT-PCR reference genes stability after glucose depletion. The total mRNA levels of three commonly used reference genes were measured by qRT-PCR and normalized to spike-in RNA control as described in Materials and Methods. Error bars, Mean ± SEM. (B) Fold changes of total candidate mRNA levels after glucose depletion were determined by qRT-PCR using *ACT1* as reference. Group I: non-mitochondria-related candidates. Group II: mitochondria-related candidates. Error bars, Mean ± SEM.

and stability of mRNAs within P-bodies depend on individual properties, and that mRNAs acting in the same process might be co-regulated.

Next, we asked whether the fate of an mRNA has an impact on its translation product. Therefore, we assessed the protein level of Tpi1p and Rlm1 (Group I) as well as Atp11p and Mrpl38p (Group II) upon glucose depletion over time (Figure 3C). Consistent with the changes in mRNA levels, Group I protein levels dropped, while the Group II protein levels remained stable or increased over the glucose starvation time course. Our results reveal distinct and separable roles of P-bodies in regulating mRNA stabilities. On one hand, P-bodies contain transcripts undergoing decay in an individually regulated time-dependent manner. On the other hand, another group of mRNAs, whose protein product contributes to stress response, are protected by P-bodies.

Puf5p contributes to both recruitment and decay of P-body mRNAs

Next, we aimed to record the transport of mRNAs into P-bodies by live-cell imaging using the well-established MS2 and U1A systems (Chung and Takizawa, 2011; Zenklusen et al., 2007). Tagging transcripts with U1A stem loops massively induced P-body formation under non-stress conditions (data not shown). Similarly, appending candidate transcripts with MS2 loops increased the co-localization of mRNA and P-body components to almost 100% (Figure 4- Figure Supplement 1), which is in marked contrast to the FISH data. This high degree of co-localization can be explained by the recent finding that highly repetitive stem-loops can lead to non-degradable 3' mRNA fragments causing mislocalization of tagged mRNAs (Garcia and Parker, 2015). Considering the strong discrepancy between the FISH and MS2 localization data in terms of extent of P-body localization, and the recently published potential aberrant localization of MS2-tagged mRNAs, we decided to use the more conservative and less errror-prone FISH-IF method to identify factors required for the localization and/or fate of mRNAs in P-bodies. We explored several known protein factors, which may contribute to this process with a candidate approach using *BSC1* (Group I) and *ATP11* (Group II) probes (Figure 4- Figure Supplement 2A). We deleted known P-body

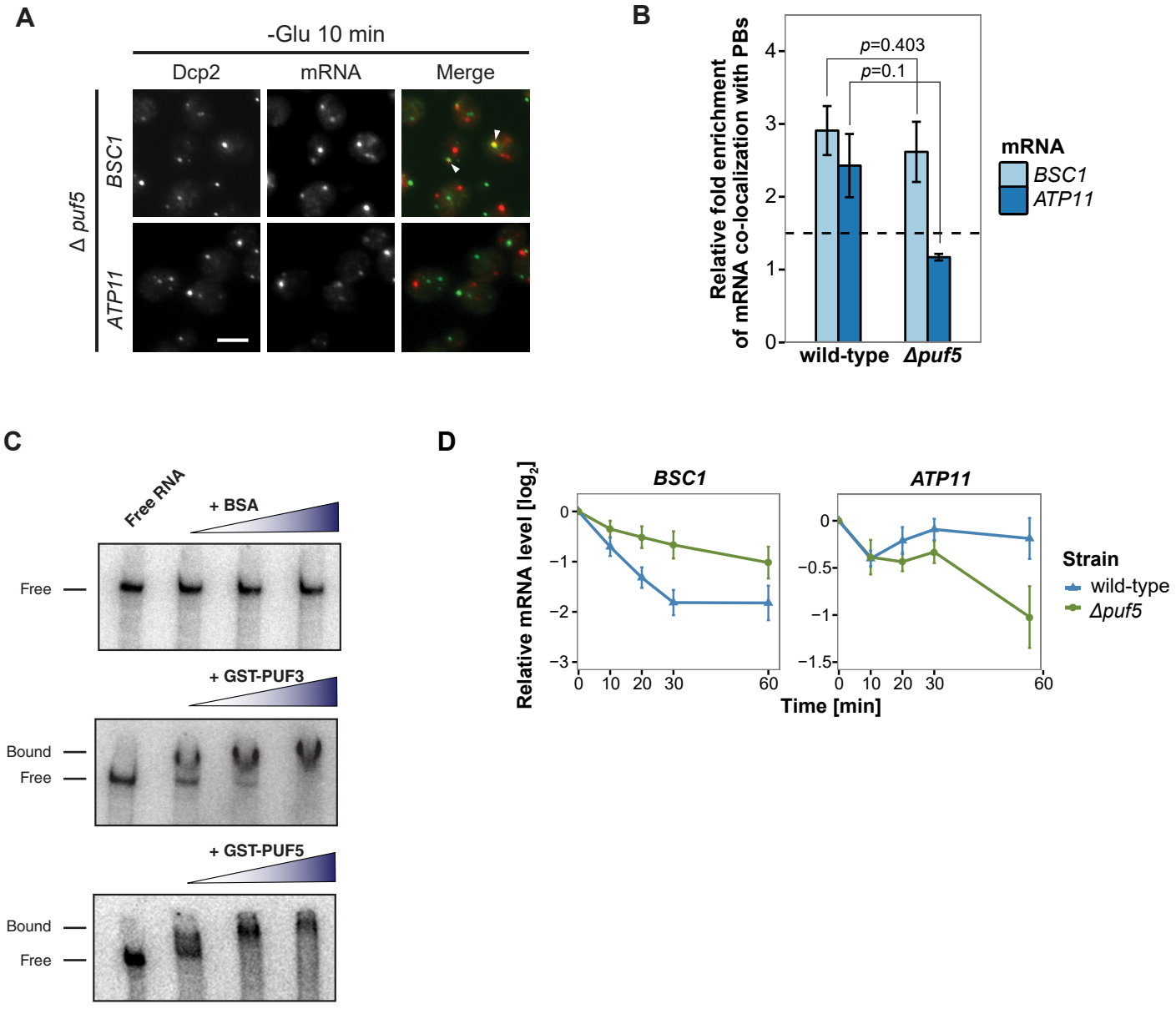

Figure 4. Puf5p is required for both mRNA recruitment and regulation of mRNA decay in P-bodies.
(A) Fluorescence images of P-bodies and *BSC1* (Group I) or *ATP11* (Group II) mRNAs following glucose depletion on Δ*puf5* cells expressing Dcp2-GFP. Scale bar, 5 μm. (B) Bar plot showing the relative fold enrichment of co-localization between *BSC1*, *ATP11* and P-bodies in Δ*puf5* strain 10 min after switched to glucose-free media. Wild type is plotted as in Figure 2C. The dashed line represents a fixed threshold of 1.5 for determining significant enrichment. Error bars, Mean ± SEM. A one-tailed, non-paired Student's *t*-test was used to determine *p* values. (C) EMSA assays using *ATP11* 3'UTR RNA (1-500 nt after STOP codon) oligonucleotide in the absence or presence of bovine serum albumin (1.25, 2.5, 5 μ M), GST-PUF3 (10, 50, 100 nM) and GST-PUF5 (1.25, 2.5, 5 μM). Unbound radiolabelled RNA (Free) shifts to a high molecular weight complex when bound to GST-PUF3 or GST-PUF5 (Bound), Results are representative of 3-4 independent experiments per protein. (D) The stability of 4-TU labeled *BSC1* and *ATP11* mRNAs was measured by qRT-PCR in Δ*puf5* strain at indicated time points following glucose depletion. Wild type is plotted as in Figure 3B. Error bars, Mean ± SEM.

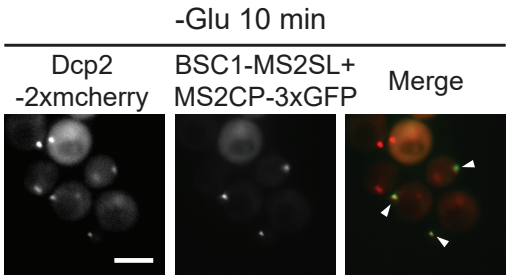

Figure 4- Figure Supplement 1. Live-cell detection of P-bodies (Dcp2-2xmcherry) and *BSC1* mRNA molecules using the MS2 system. Scale bar, 5 μm. Results are representative of 3 independent experiments.

A

Deletion strains	Fold enrichment of mRNA co-localization with PBs <1.5	
	BSC1	*ATP11*
Δ *sbp1*	-	-
Δ *khd1*	-	-
Δ *ngr1*	-	-
Δ *whi3*	-	-
Δ *pbp2*	-	-
Δ *puf3*	-	-
Δ *puf5*	-	+
Δ *puf6*	-	-

B

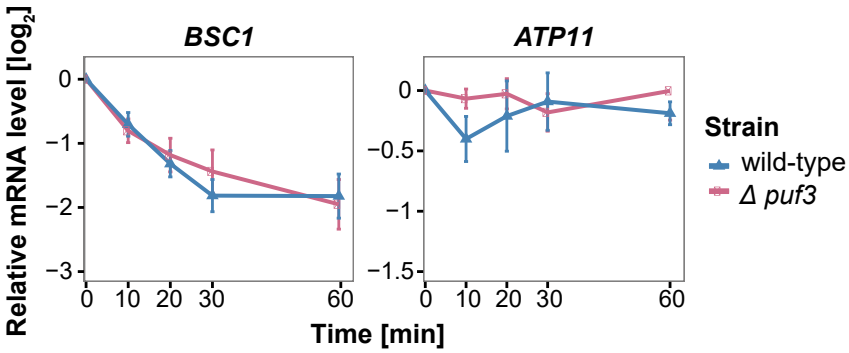

C

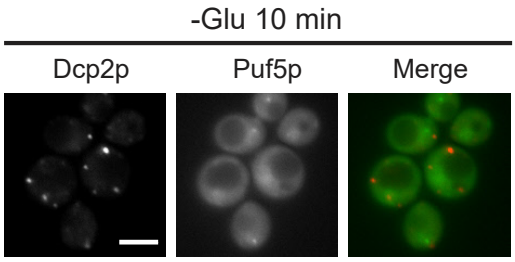

Figure 4- Figure Supplement 2. A screen for RNA-binding proteins required for mRNA recruitment to P-bodies. (A) A screen to identify RNA-binding proteins affecting mRNA recruitment to P-bodies by FISH-IF. *BSC1* and *ATP11* were selected for screening performed with the deletion strains as listed. A fold enrichment value above 1.5 was classified as not required (-), below as required (+). Two independent experiments were performed per mRNA per strain. (B) The stability of 4-TU labeled *BSC1* and *ATP11* mRNAs was measured by qRT-PCR in Δ*puf3* strain at indicated time points following glucose depletion. Wild type is plotted as in Figure 3B. Error bars, Mean ± SEM. (C) Live-cell detection of P-bodies (Dcp2-2xmcherry) and Puf5p (GFP) following glucose withdrawal, Scale bar, 5 μm. Results are representative of 3 independent experiments.

components or factors associating with P-bodies upon glucose deprivation (Sbp1p, Khd1p, Ngr1p and Whi3p) (Cai and Futcher, 2013; Mitchell et al., 2013) and candidates known to promote mRNA decay or repress mRNA translation, including poly(A)-binding protein II (Pbp2p), two PUF family proteins (Puf3p and Puf5p) and one non-canonical PUF protein (Puf6p) (Chritton and Wickens, 2010; Wickens et al., 2002). Remarkably, the loss of Puf5p efficiently inhibited the recruitment of *ATP11* to P-bodies as the co-localization dropped to background levels (Figure 4A, 4B). In contrast, *BSC1* localization was unaffected (Figure 4A, 4B). The observed lack of *ATP11* P-body localization in *Δpuf5* cells was specific, since none of the other deletion strains showed a targeting defect (Figure 4- Figure Supplement 2A). To investigate the consequence of the inability of *ATP11* to be protected in P-bodies in Δ*puf5*, we determined the *ATP11* mRNA levels. Indeed, *ATP11* mRNA levels declined, when no longer associated with P-bodies (Figure 4C). These data confirm that *ATP11* mRNA is protected in P-bodies from decay.

Conversely, the localization of *BSC1* mRNA to P-bodies was not altered in cells lacking Puf5p and the mRNA seemed to be stabilized to a certain degree, consistent with Puf5p's role in mRNA decay (Goldstrohm et al., 2006). Recent data suggest that Puf5p binds to both *BSC1* and *TPI1* mRNA, but not to any of the candidates of Group II (Wilinski et al., 2015). In contrast, *ATP11* has been reported to be a target of Puf3p (Gerber et al., 2004). However, in ∆*puf3* neither the localization to P-bodies nor *ATP11* stability was affected, suggesting Puf3p is presumably not essential for P-body related *ATP11* regulation upon glucose deprevation (Figure 4- Figure Supplement 2B). Even though, others and we were unable to detect Puf5p in P-bodies (Figure 4- Figure Supplement 2C) (Goldstrohm et al., 2006), it is still possible that Puf5p interacts with *ATG11*. To address this possibility, we performed electro mobility shift assays (EMSAs) with 500 bp of the *ATP11* 3'UTR and Puf3p and Puf5p. (Figure 4D). Both Puf3p and Puf5p, but not BSA bound the *ATP11* 3'UTR, albeit the Puf5p binding affinity being much weaker. Neither *ATP11* nor any of the other Group II mRNAs tested, contains a recognizable Puf5-binding sequence,

255 indicating the presence of a non-canonical binding site. Our data suggest that Puf5p directly
256 controls *BSC1* and *ATP11* mRNA stability and *ATP11* mRNA localization.

257 **The 3'UTR is necessary but not sufficient for mRNA targeting to P-bodies**

258 Considering that the 3'UTR of mRNAs contains most regulatory elements, which often have an
259 important role in determining mRNA localization (Andreassi and Riccio, 2009; Vuppalanchi et al.,
260 2010), we next investigated whether 3'UTRs play a role in mRNA targeting to P-bodies. We
261 replaced the endogenous 3'UTR of *BSC1* and *ATP11* with the 3'UTR of *K. lactis TRP1* (*klTRP1*)
262 and examined the localization of the chimera by FISH-IF after glucose starvation (Figure 5A).
263 Replacing the 3'UTR abolished recruitment of both mRNAs to P-bodies (Figure 5B, 5C),
264 suggesting that even though the localization signal must be different between *ATP11* and *BSC1*,
265 the necessary sequences are present in the 3'UTR. Consistent with the mislocalization, *BSC1*
266 and *ATP11* transcripts were stabilized and degraded, respectively (Figure 5D). The destabilization
267 of the *ATP11* mRNA is also reflected in the reduction of Atp11p protein levels under the same
268 conditions. Thus, the 3'UTR is essential for the fate and P-body localization under glucose
269 starvation for both transcripts.

270 Since the 3'UTR was essential for both mRNAs, we investigated whether common primary
271 sequence motifs between all mRNAs, which were specifically enriched in P-bodies under a unique
272 stress, exist using the MEME Suite (Bailey et al., 2009). Probably not so unexpected, we did not
273 find any significant primary sequence conservations or enrichment, of any particular motif. Next,
274 we clustered stress-dependent P-body mRNAs based on secondary structures within the 3'UTR
275 using NoFold (Middleton and Kim, 2014). In comparison to non-candidate mRNAs, each stress-
276 specific candidate set contained 10-20 clusters of transcripts that were differentially enriched in
277 certain structure motifs (Table S2). Interestingly, enriched motifs exhibited strong similarities (Z-
278 score > 3) to known miRNA motifs from RFAM, in line with the observation that at least in
279 mammalian cells and *Drosophila*, P-bodies were shown to contain miRNA silencing complex
280 components (Liu et al., 2005; Sen and Blau, 2005). One possible explanation is that general stem-

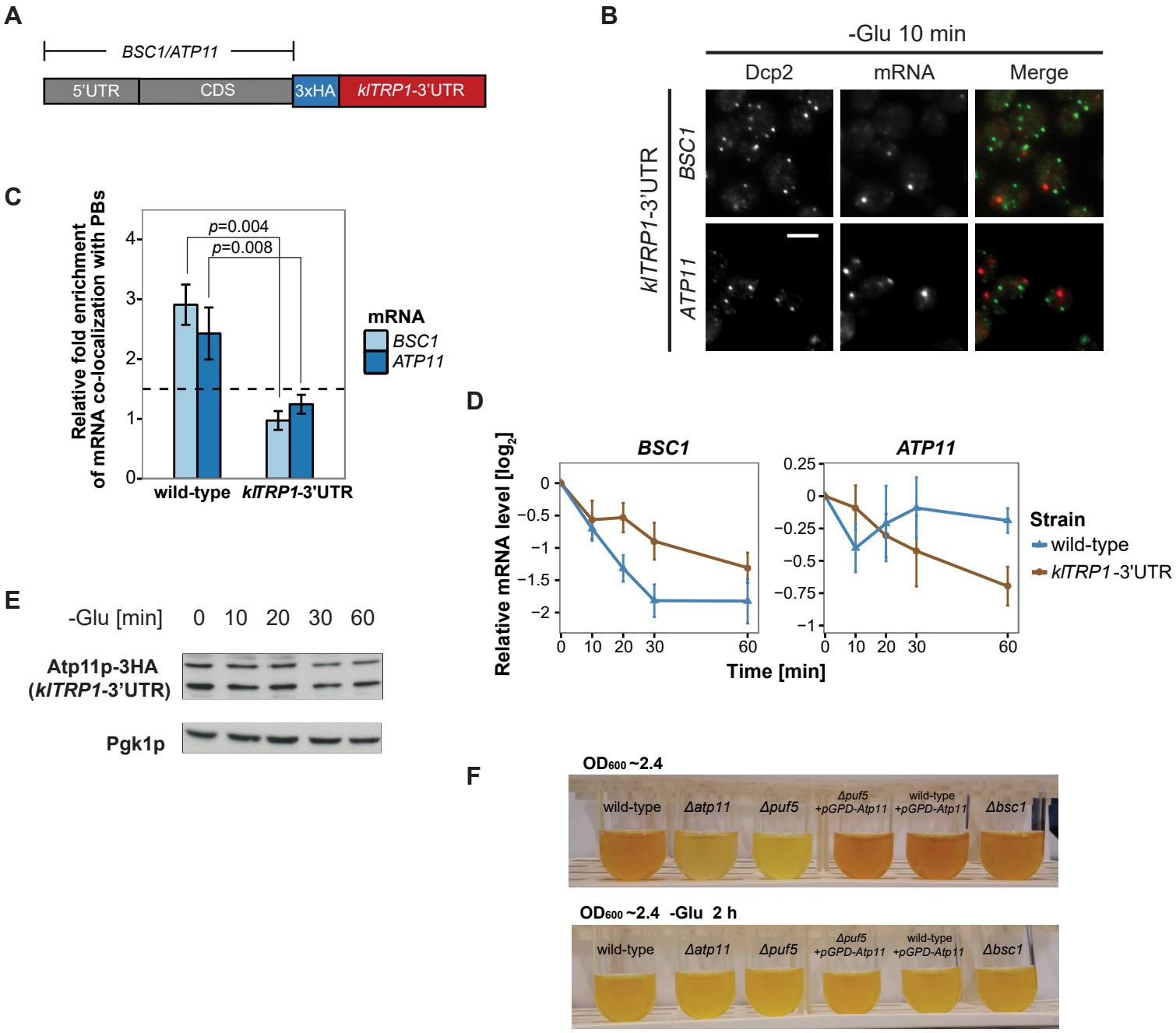

Figure 5. 3'UTR is necessary for mRNA localization to P-bodies.
(A) A schematic representation of C terminal tagging with 3x HA. The endogenous 3'UTR was simultaneously replaced by the 3'UTR of *klTRP1*. (B) Fluorescence images of P-bodies and *BSC1*, *ATP11* mRNAs following glucose depletion on corresponding 3'UTR replaced strains. Scale bar, 5 μm. (C) Bar plot depicting the relative fold enrichment of co-localization between *BSC1*, *ATP11* and P-bodies in corresponding 3'UTR replaced strains 10 min after glucose starvation. Wild type is plotted as in Figure 2C. The dashed line represents a fixed threshold of 1.5 for determining significant enrichment. Error bars, Mean ± SEM. A one-tailed, non-paired Student's *t*-test was used to determine *p* values. (D) The stability of 4TU labeled *BSC1* and *ATP11* mRNAs was determined by qRT-PCR in corresponding 3'UTR replaced strains at indicated time points following glucose depletion. Wild type is plotted as in Figure 3B. Error bars, Mean ± SEM. (E) Western blot analysis of Atp11-HA (*klTRP1* 3'UTR) at indicated time points after glucose deprivation. Pgk1 was used as a loading control. Anti-HA and anti-Pgk1p were used for detection. Results are representative of 3 independent experiments. (F) Assessment of intracellular glycogen content in wild type, *ATP11*, *PUF5* deletion strains in the absence or presence of *ATP11* overexpression plasmid and *BSC1* deletion strain by iodine staining. Yeast cultures were grown to stationary phase (OD_{600} ~2.4) in medium containing 2% dextrose (upper panel). Then cells were shifted to medium without dextrose for 1 h (lower panel). Results are representative of 4 independent experiments.

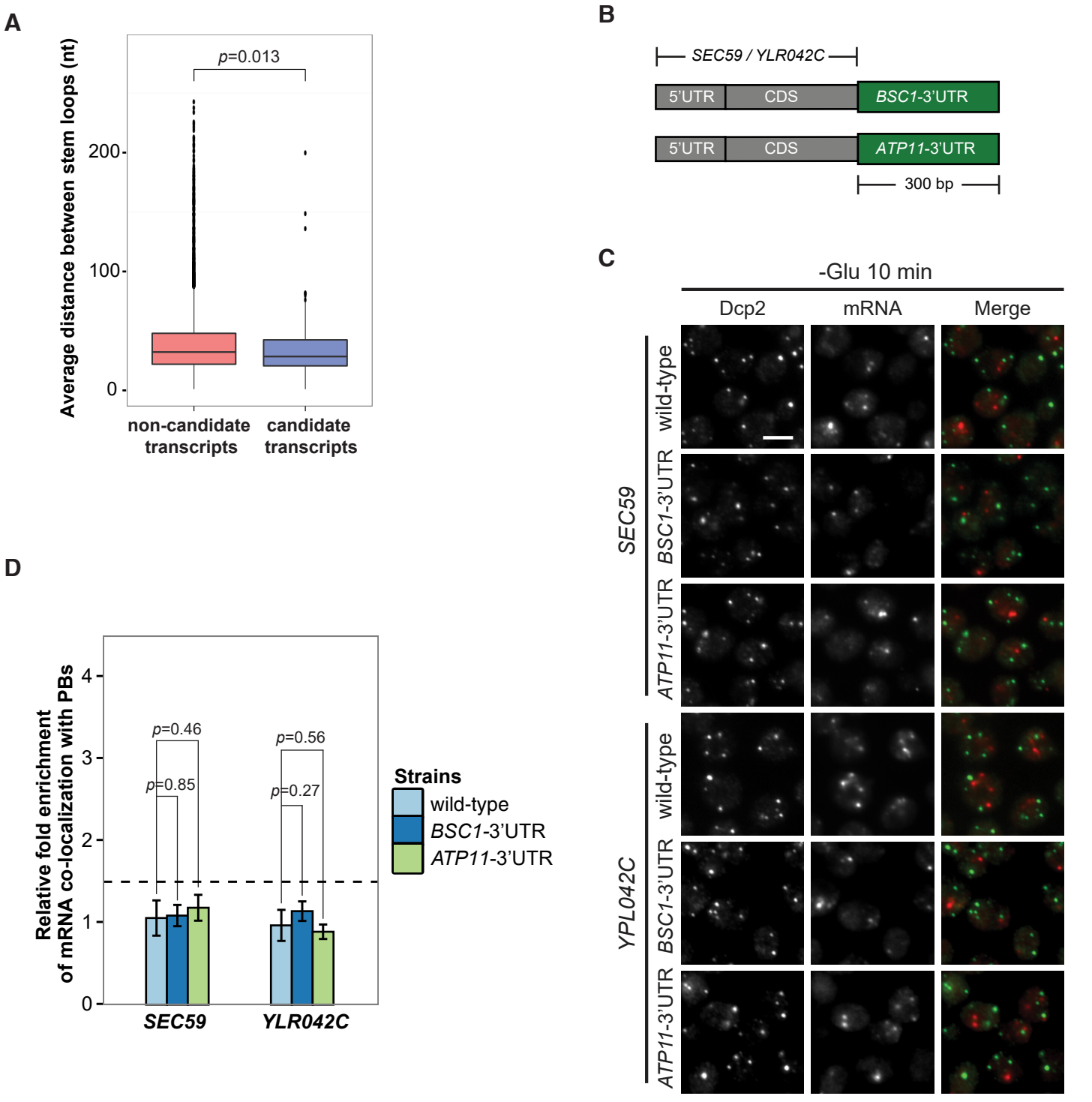

Figure 5- Figure Supplement 1. 3'UTR is insufficient for mRNA localization to P-bodies.
(A) Box plot of average distances between stem loops among the 3'UTRs of candidate transcripts versus non-candidate transcripts. A non-parametric, one-sided Wilcoxon rank-sum test was used to determine *p* values. (B) A schematic representation of 3'UTR transplantation chimeras. The endogenous 3'UTRs (300 bp downstream from stop codon) of *SEC59* and *YLR042C* (300 bp downstream from stop codon) were replaced by the 3'UTRs of *BSC1* and *ATP11*, respectively. (C) Fluorescence images of P-bodies and *SEC59* and *YLR042C* mRNAs following glucose depletion. Scale bar, 5 μm. (D) Bar plot showing the relative fold enrichment of co-localization between *SEC59*, *YLR042C* and P-bodies in indicated chimeric strains 10 min after glucose withdrawal. Wild type is plotted as in Figure 2C. The dashed line represents a fixed threshold of 1.5 for determining significant enrichment. Error bars, Mean ± SEM. A one-tailed, non-paired Student's *t*-test was used to determine *p* values.

loop structures may favor P-body localization under stress. To test this hypothesis, we determined the predicted number of stem loops in the 3'UTR of mRNAs enriched specifically under stress versus inert mRNAs and calculated the distance between stem loops. We observed a decrease in the distance between stem loops, suggesting clustering of the loops (Figure 5- Figure Supplement 1A). To determine whether clusters of stem loops would be sufficient to drive P-body localization, we transplanted the 3'UTR of *BSC1* or *ATP11* to a non-P-body associated transcript *SEC59* and a sodium specific P-body-associated transcript *YLR042C* (Figure 5- Figure Supplement 1B). None of the four chimaeras recapitulated the localization of native *BSC1* and *ATP11* transcripts under stress (Figure 5- Figure Supplement 1C, 1D). Thus, although the 3'UTRs are essential, they are not sufficient by themselves to drive mRNA transport into P-bodies. Most likely other elements in the coding sequence and/or 5'UTR act cooperatively.

Overexpression of *ATP11* rescues the glycogen accumulation deficiency in Δ*puf5* cells

Finally, we asked whether the stabilization of *ATP11* mRNA by Puf5p is beneficial for the cell. Puf5 promotes chronological lifespan (Stewart et al., 2007), which is dependent on the accumulation of carbohydrates such as glycogen (Cao et al., 2016). Likewise, a Δ*atp11* strain showed decreased glycogen accumulation (Wilson et al., 2002). Therefore, we asked whether Atp11p levels would contribute to the Puf5p ability to promote lifespan and stained for glycogen when cells reached stationary phase. As expected Δ*atp11* and Δ*puf5* failed to efficiently accumulate glycogen as indicated by the absence of the brown color (Figure 5F). Importantly overexpression of *ATP11* in the Δ*puf5* strain was sufficient to restore glycogen accumulation, suggesting that the stabilization of *ATP11* mRNA by Puf5p contributes to Puf5p's positive effect on chronological lifespan.

Discussion

The fate of mRNAs and its regulation under different stress conditions is still not well understood. mRNAs have been proposed to be either associated with ribosomes or stored/decayed in P-bodies and SG. Here we demonstrate that the content and the fate of mRNA in P-bodies is stress-dependent, varying from decay to stabilization. We furthermore provide evidence that different mRNA classes use different mechanisms to be P-body localized. The localization and fate of these mRNAs are dependent on interactions with RNA binding proteins such as Puf5p and essential information present in the 3'UTR of the mRNA.

To enable this analysis, we first devised a method to enrich RNPs based on *in vivo* chemical cross-linking followed by streptavidin affinity purification. This method allows the identification and global analysis of P-body associated mRNAs. We previously used a similar approach to successfully discover a novel exomer-dependent cargo (Ritz et al., 2014) and a novel facultative P-body component (Weidner et al., 2014). We improved the procedure permitting the reliable enrichment and detection of mRNAs associated with P-bodies under a variety of stress conditions. Moreover, our method works regardless of poly(A) tail length or partial transcript degradation, and hence could be applied for the identification of many types of RNAs. Moreover, this method would also be applicable to study protein-DNA interactions.

We mostly concentrated our further analysis on hits from the glucose starvation experiments but it is very likely that these findings can be generalized to other stresses. We identified three classes of mRNAs in P-bodies. The first class consists of mRNAs that are generally deposited into P-bodies, independent of the stressor. We did not investigate their fate further in this study, but we assume that most of those transcripts would be prone to decay. The second class contains mRNAs that are stressor-dependent and decayed. It is important to note that the decay rate of mRNAs in this class is very variable and could represent an intrinsic property of the mRNA or a subset of mRNAs. Some transcripts will be decayed almost immediately after

arrival in P-bodies, while others are initially excluded from degradation. The kinetics of decay also appears to vary, indicating that even within P-bodies the degradation of client RNAs is highly regulated. Finally, the third class corresponds to mRNAs that are also stress-specific, but stabilized, rather than degraded. It appears as if this class is enriched in transcripts whose products would be beneficial for stress survival. This hypothesis is based on the stabilization of transcripts involved in mitochondrial function under glucose starvation, a condition under which mitochondria are up-regulated (Wu et al., 2004). Thus, P-bodies emerge as context-dependent regulator in stress responses. Although P-bodies have been proposed previously as mRNA decay and storage organelles (Sheth and Parker, 2003), the studies on which this model was based had either been performed on very few selected transcripts or artificial transcripts with extended G-tracts driving P-body localization through imaging or genome-wide analyses, taking all the mRNAs present in a lysate into account (Arribere et al., 2011; Brengues et al., 2005; Sun et al., 2013). Our approach is different in that we enrich first for P-bodies and then extract the RNA specifically from the P-body fraction. Therefore, our data provide an unprecedented wealth of information on the mRNA content and fate within P-bodies.

Since the fate of an mRNA is stressor-dependent, it is tempting to speculate that the different mRNA classes are recruited to P-bodies through different pathways. In support of this hypothesis, we identified the RNA binding protein Puf5p as a protein regulating both the localization of on transcript as well as the degradation of another (Figure 6). The latter function is easily explained by the established role of Puf5p as interactor of the Crr4/Not deadenylation complex, which shortens the poly(A)-tail independent of the subsequent route of destruction through P-bodies or exosomes (Balagopal et al., 2012). In fact, *BSC1* mRNA was recently identified as Puf5p target (Wilinski et al., 2015). In the absence of Puf5p, *ATP11* is no longer P-body localized and is destabilized. Hence, in this case P-bodies protect an mRNA from degradation in a Puf5p-dependent manner. It is striking, however, that Puf5p possesses this dual

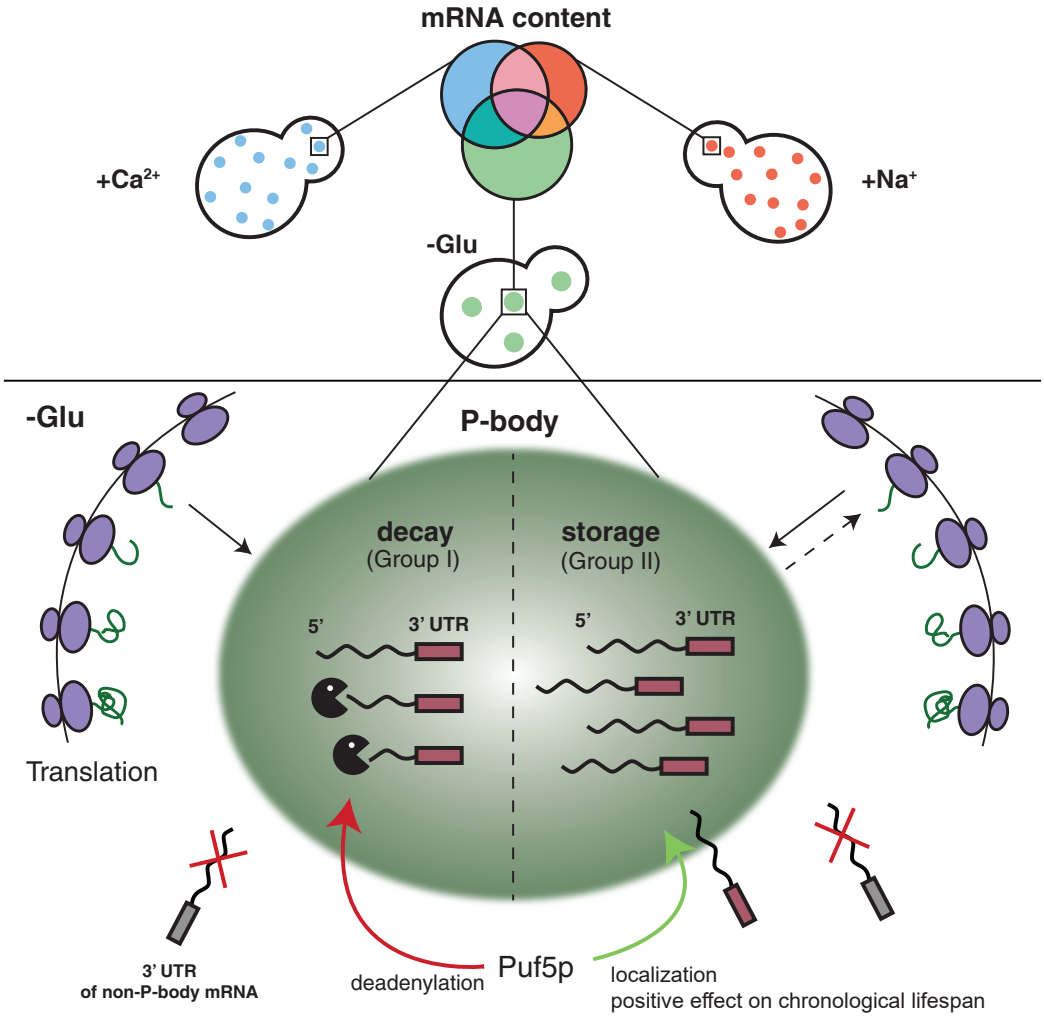

Figure 6. Schematic model summarizing our findings.

role of protection and destruction depending on the mRNA, as well as being involved in the localization of mRNAs to P-bodies.

The notion that mRNAs are decayed in P-bodies was recently challenged (Pelechano et al., 2015; Sweet et al., 2012). Instead, it was suggested that decay might mostly happen co-translationally. We cannot exclude that a part of the RNAs is degraded co-translationally, since the decay machinery in both processes appears to be identical. In favor of mRNA decay in P-bodies, we confirmed hits from the biochemical enrichment procedure by *in vivo* localization studies. We found that P-body-localized mRNAs were degraded with different kinetics. Moreover, we would expect to find significantly higher sequence coverage of the 3' region of candidate mRNAs, which we did not observe. Also, the fate -stabilization versus degradation- of *BSC1* in a Puf5p-dependent manner, which was not accompanied by modulating P-body localization, is in support of P-body as decay compartment. Thus, our data are consistent with mRNA degradation in P-bodies under stress conditions. In contrast, *ATP11* may become a co-translational degradation target in the absence of Puf5p. However co-translational mRNA decay might still be a major pathway in non-stressed cells, in which microscopically P-bodies are not frequently detected. At least the 5' decay machinery, the helicase Dhh1p and the 5'exonuclease Xrn1p have been found to be associated with polysomes also in the absence of a stressor (Pelechano et al., 2015; Sweet et al., 2012; Weidner et al., 2014).

Our findings demonstrate that P-body associated mRNA can follow different fates, namely decay or stabilization. Whether these two functions are performed by the same or different P-bodies remains unclear. We favor the possibility, however, that both functions can be provided by the same P-body. Recent data from *Drosophila* sponge bodies, which are the equivalent of P-bodies in embryos, suggest that the degradation and decay may happen in the same compartment (Weil et al., 2012). Likewise, there is no evidence thus far for differential protein composition of P-bodies formed under the same stress condition (Kulkarni et al., 2010). Although,

382 it is possible that the transient protein components may vary from one another, we expect the
383 major factors would be discriminative to fulfill opposing functions and mRNA selectivity.

384 Stabilized mRNAs may return into the translation competent pool. Whether this re-initiation
385 would be through diffusion of the mRNA from the P-body into the cytoplasm or through another
386 organelle, such as stress granules (SG), remains to be established. SGs harbor stalled translation
387 initiation complexes, whose formation can also be triggered upon a variety of stresses.
388 Additionally, SGs frequently dock and fuse with P-bodies, and they share some common protein
389 factors (Buchan et al., 2008; Buchan et al., 2011; Kedersha et al., 2005; Stoecklin and Kedersha,
390 2013). As mRNAs in SGs are polyadenylated, they are not subject to immediate degradation
391 (Kedersha et al., 1999; Stoecklin and Kedersha, 2013). Based on those evidences, we speculate
392 that the re-engagement of stable transcripts into translation is likely mediated via SGs.

393 A number of genome-wide studies detailing responses to stress have been performed
394 (Miller et al., 2011; Munchel et al., 2011). Most of the studies deal with global RNA synthesis and
395 decay, but do not provide any insights into the regulated storage of mRNA. In this study, we
396 addressed this issue and uncovered Puf5 as key molecule in the decision making whether or not
397 a particular mRNA must be degraded under glucose starvation. This decision making explains
398 Puf5p's positive effect on chronological lifespan, as increasing Atp11p levels were sufficient to
399 rescue the glycogen accumulation defect of Δ*puf5* cells. How the decision making is brought about
400 will be the focus of future studies.

401

402

403

404

405

406

407

Materials and Methods

Yeast strains and growth conditions

Standard genetic techniques were employed throughout (Sherman, 1991). Unless otherwise noted, all genetic modifications were carried out chromosomally. Chromosomal tagging and deletions were performed as described (Janke et al., 2004; Knop et al., 1999). For C-terminal tagging with 3xHA, the plasmid pYM-3HA (*klTRP1*) and with 9xmyc the plasmid pOM20 (*kanMX6*) and pSH47 (*URA3*) were used. The use of pOM plasmids (Gauss et al., 2005) in combination with Cre recombinase allowed C-terminal chromosomal tagging and preservation of the endogenous 3'UTR at the same time. The plasmid pFA6a-natNT2 was used for construction of all deletion strains, except for *Δpuf3* (pUG73), Δ*atp11* and Δ*bsc1* (pUG72). 3'UTR transplantation experiments were carried out with the *Delitto Perfetto* method using the pCORE plasmid (*kanMX4-URA3*) (Storici and Resnick, 2006).

For C-terminal tagging Puf5p with GFP, the plasmid pYM26 (*klTRP1*) was used. pFA6a-3xmcherry (*hphNT1*) plasmid was used in tagging Dcp2p with mcherry (Maeder et al., 2007). For live-cell mRNA imaging, MS2SL tagged strains were constructed using pDZ415 (24MS2SL loxP-Kan-loxP). To remove selection marker and visualize the transcripts, the Cre recombinase-containing plasmid pSH47 (URA3) and MS2SL coat protein expressing plasmid pDZ274 (pLEU MET25pro MCP-2x-yeGFP) were co-transformed into cells afterwards (Hocine et al., 2013). Plasmids pDZ415 (Addgene plasmid # 45162) and pDZ274 (Addgene plasmid # 45929) were gifts from Robert Singer and Daniel Zenklusen (Albert Einstein College of Medicine, Bronx, NY, USA). Primers and strains used in this study are listed in Table S3 and S4.

Unless otherwise noted, yeast cells were grown in YPD (1% yeast extract, 2% peptone, 2% dextrose) at 30˚C. For glucose deprivation, cultures were further grown in YP media without dextrose for indicated times. For mild osmotic stress, YPD growth medium was supplemented with 0.5 M NaCl or 0.2 M $CaCl_2$ for indicated times. Yeast cells were harvested at mid-log phase (OD_{600} of 0.4-0.8).

434 **Chemical cross-linking coupled to affinity Purification (cCLAP) and preparation of RNA-**
435 **Seq samples**

436 The cCLAP was carried out according to Tagwerker et al. (2006), Hafner et al. (2010) and Kishore
437 et al. (2011) with modifications. Cells expressing Dcp2-HBH or Scd6-HBH were grown to mid-log
438 phase, subjected to the corresponding stress and crosslinked with 1% formaldehyde for 2 min.
439 Control cells were treated equally except stress application. Cells were lysed in RIPA buffer
440 (50 mM Tris-HCl pH 8.0, 150 mM NaCl, 1% NP-40, 0.5% sodium deoxycholate, 0.1% SDS,
441 supplemented with protease inhibitors) using FastPrep (MP Biomedicals). To dissolve large RNPs,
442 supernatants were treated with 50 U/ml RNase T1 (Fermentas) at 22°C for 15 min. Pull-downs
443 were performed with streptavidin agarose beads (Thermo Fisher Scientific) in binding buffer
444 (50 mM NaPi pH 8.0, 300 mM NaCl, 6 M GuHCl, 0.5% Tween-20). The second RNase T1
445 digestion was performed on the beads with a final concentration of 1 U/µl. Radiolabeling of RNA
446 was performed by adding 0.5 µCi/µl γ-^{32}P-ATP (Hartmann analytic) and 1 U/µl T4 PNK (New
447 England Biolabs). To purify RNA, proteins were digested using 1.2 mg/ml proteinase K (Roche)
448 in 2 x proteinase K buffer (100 mM Tris-HCl pH 7.5, 200 mM NaCl, 2 mM EDTA, 1% SDS) for
449 30 min at 55˚C. The RNA was subsequently isolated using phenol-chloroform-isoamyl alcohol
450 (125:24:1) (Sigma-Aldrich) as described (Schmitt et al., 1990). Purified RNA was subjected to 3'
451 and 5' adapter ligation following Illumina's TruSeq Small RNA Library Prep Guide. To reduce the
452 rRNA species, RiboMinus transcriptome isolation kit (Invitrogen) was used according to the
453 manufacturer's protocol. Reverse transcription using SuperScript III reverse transcriptase
454 (Invitrogen), oligo-dT and random hexamer was performed afterwards. The cDNA libraries were
455 generated by a final PCR amplification step with Ilumina indexing primer (RPI1-4, Table S2).
456 In this study, five library sets (from five biological replicates) were sequenced. Except the first
457 library set, all the libraries were generated as described above. In the first library set, the
458 radiolabeling step was omitted and the PAGE purification steps were replaced by column-based
459 purification with RNeasy kit (Qiagen), according to the manufacturer's instruction.

460 **Processing of small RNA-Seq reads**

461 RNA-Seq libraries were sequenced on Illumina HiSeq2000 with single read to 50 bp reads. We
462 clipped adapters and trimmed low quality bases using Trimmomatic version 0.30 (Bolger et al.,
463 2014) with parameters "SE –s phred33 ILLUMINACLIP:Illumina_smallRNA_adapters.fa:20:5:30
464 LEADING:30 TRAILING:30 MINLEN:10", where Illumina_smallRNA_adapters.fa contained all
465 adapter and primer sequences from the TruSeq Small RNA Sample Preparation Kit.
466 Subsequently, reads were aligned to Saccharomyces cerevisiae genome EF4.72 from ENSEMBL
467 using Bowtie version 1.0.0 (Langmead et al., 2009) with parameters "-n 0 –l 28 –e 70 –k1 –m 1 -
468 -best --strata --sam --nomaqround". Reads were counted per exon using htseq-count (Anders et
469 al., 2015) with default parameters against ENSEMBL's matching GTF file for EF4.72 and
470 aggregated on the gene-level.

471 **Analysis of P-body enriched mRNAs**

472 Analysis of P-body enriched mRNAs was performed using edgeR version 3.0 (Robinson et al.,
473 2010) using standard procedures for count normalization and estimation of dispersion. The gel
474 label and batch were included as factors in the experimental design (Table S5). We identified
475 significant (p<0.05) upregulated mRNAs exclusive for each stress condition by testing each
476 individual stress condition against the wild type condition and removing those mRNAs that were
477 identified as common hits when testing the joint set of stress conditions against unstressed control.
478 For glucose depletion stress, we additionally excluded genes previously shown to be significantly
479 enriched in polysomes (Arribere et al., 2011) for the same stress.

480 **Gene Ontology (GO) term enrichment analysis**

481 P-body enriched mRNAs for each stress condition were tested for GO biological processes (BP)
482 enrichment using hypergeometric tests as implemented in the hyperGTest function from the
483 GOstats R/Bioconductor package version 1.7.4. The mRNA universe was defined for each stress
484 condition as the set of mRNAs with a mean expression over all replicates larger than or equal to
485 the first quartile. For GO term mRNA annotation, the R/Bioconductor package org.Sc.sgd.db

version 3.1.2 was used. P-values from the hypergeometric tests were visualized using the ggplot2 R package version 1.0.1.

Combined fluorescence in situ hybridization (FISH) and immunofluorescence (IF)

Combined FISH and IF was performed as described (Kilchert et al., 2010; Takizawa et al., 1997). The following antibodies and solution were used for detection: anti-DIG-POD (Roche, 1:750 in PBTB), anti-HA (Eurogentec HA11; 1:250), anti-GFP (Roche GFP clones 7.1 and 13.1, 1:250), goat anti-mouse-IgG-Alexa488 (Invitrogen, 1:400 in PBS) and tyramide solution (PerkinElmer, 1:100 in Amplification Solution supplied with kit). Primers with T7 promoter ends (Table S3) and MEGAscript T7 transcription kit (Ambion) were used for probe generation. To obtain fluorescence images, slides were mounted with Citifluor AF1 (Citifluor), supplemented with 1 µg/ml DAPI to stain the nuclei. Images were acquired with an Axiocam MRm camera mounted on an Axioplan 2 fluorescence microscope using a Plan Apochromat 63x/NA1.40 objective and filters for eqFP611 and GFP. Axiovision software 3.1 to 4.8 was used to process images (Carl Zeiss).

Co-localization analysis

Signals of P-bodies and mRNA were identified using the spots tools in Imaris software package (Bitplane). For co-localization determination, the MATLAB (MathWorks)- Imaris plug-in “co-localize spots” function was used with a threshold of 50% of the distance between centers of two spots. The percentage of mRNA co-localization with P-bodies was calculated by dividing co-localized FISH spots by total FISH spots. Approximately 200 cells from at least three biologically independent experiments were counted per mRNA per condition.

Pulse-chase labeling with 4TU and RNA purification

The pulse-chase labeling experiment was carried out as described previously (Zeiner et al., 2008). For the pulse, yeast culture was grown in HC-Ura drop-out media supplemented with 2% dextrose, 0.1 mM uracil and 0.2 mM 4-Thiouracil (Sigma-Aldrich) for 6 h. Yeast were spun down at 3,000 g for 2 min and resuspended in HC-Ura drop-out media containing 20 mM uracil (chase). Afterwards, yeasts were collected by centrifugation at the following time points: t = 0, 10, 20, 30,

and 60 min. Cells were lysed followed by total RNA isolation using phenol-chloroform-isoamyl alcohol (125:24:1) (Sigma-Aldrich) as described (Schmitt et al., 1990). The RNA was then subjected to biotinylation and further purification according to Zeiner et al. (2008).

The same pulse-chase labeling protocol was performed to determine the mRNA stability of *ACT1*, *PGK1* and *RPL37b* under glucose deprivation condition, and 200 pg humanized Renilla luciferase (*hRLuc*) RNA spike-in was added per microgram total RNA as reference gene. The same RNA purification protocol was followed to isolate 4TU labeled RNA as well as total RNA. At least three biologically independent pulse-chase experiments per mRNA per strain were performed.

Quantitative RT-PCR

0.5-1 µg of 4-TU labeled RNA or total RNA was reverse transcribed with the Transcriptor reverse transcriptase kit (Roche), oligo-dTs and random hexamers. The mRNA levels were analyzed by SYBR green incorporation using ABI StepOne Plus real-time PCR system (Applied Biosystems). Primers used in qRT-PCR are listed in Table S3.

Western Blotting

Glucose deprived cells were harvested at indicated times. For each time point, 9 ml of culture was collected, immediately treated with cold trichloroacetic acid (10% final concentration), and incubated on ice for 5 min. Yeast extracts were prepared as described (Stracka et al., 2014). The protein concentration was determined using the DC Protein Assay (Bio-Rad), and the total lysate was analyzed by SDS-PAGE and immunoblotting. The following antibodies were used for immunoblotting: anti-Tpi1p (LSBio LS-C147665; 1:5,000); anti-Atp11p (a gift from Sharon H. Ackerman, Wayne State University, Detroit, MI); anti-HA (Eurogentec HA11; 1:1,000); anti-myc (M4439; Sigma-Aldrich; 1:1,000); anti-Pgk1p (Invitrogen #A-6457; 1:1,000). Enhanced Chemiluminescence (ECL; GE Healthcare) was used for detection.

538 **Live-cell imaging**

539 For live-cell imaging with MS2 system. Yeast cells were grown in HC-Leu medium containing 2%
540 glucose to mid-log phase. The cells were taken up in glucose-free HC-Leu medium afterwards.
541 For live-cell imaging with Dcp2p and Pufp, Yeast cells were grown in YPD medium to mid-log
542 phase, and resuspended in HC-complete medium lacking glucose. Fluorescence was monitored
543 as described in FISH-IF.

544 **Electrophoretic mobility shift assays (EMSA)**

545 Recombinant GST-PUF3 (amino acids 465-879) and GST-PUF5 (amino acids 126–626)
546 expressed form pWO12 and pWO18 (Gifts from Wendy M. Olivas, University of Missouri St. Louis,
547 St. Louis, MO), respectively were purified and stored in 50mM Tris/HCl pH 8.0, 10% glycerol. The
548 *ATP11* 3'UTR RNA (1-500 nt after STOP codon) was transcribed from a template containing T7
549 RNA polymerase promoter with MEGAscript T7 transcription kit (Ambion) and α-^{32}P-UTP
550 (10mCi/ml). Binding reactions (20 µL) contained 4,000 cpm of labelled RNA, varying
551 concentrations of protein, 20 U RNasin Plus RNase Inhibitor (Promega) and 1 x binding buffer
552 (10 mM Tris/HCl pH 7.5, 100 mM KCl, 1 mM EDTA, 0.1 mM DTT, 0.01 mg/ml bovine serum
553 albumin, 5% glycerol). Reactions were incubated at RT for 30 min, and separated on a 4% non-
554 denaturing acrylamide gel. Gels were dried, exposed to a phosphor screen for 10-16 hours, and
555 the screens scanned using a phosphorimager (Typhoon FLA 7000, GE Healthcare).

556 **Identification of secondary structure motifs within the 3'UTRs of P-Body-associated**
557 **mRNAs**

558 Secondary structure motifs in the 3' untranslated regions (UTRs) of transcripts, overrepresented
559 among differentially enriched mRNAs for each stress condition, were identified using NoFold
560 (Middleton and Kim, 2014) version 1.0. 3' UTR sequences were extracted from the biomart
561 (http://biomart.org) by selecting 300 base pairs (bp) downstream of the coding sequence (CDS).
562 The internal NoFold boundary file bounds_300seq.txt was used along with a file containing UTR

563 sequences of all non-enriched mRNAs as a background for enrichment analysis and parameter -
564 -rnaz. All other parameters were used in the default setting.

565 **Analysis of intracellular glycogen**

566 Glycogen content in yeast cells was visualized using iodine staining (Quain and Tubb, 1983). Wild
567 type, Dcp2-GFP Δ*atp11,* Dcp2-GFP Δ*puf5* and Dcp2-GFP Δ*bsc1* strains were grown in HC
568 medium, and strains containing the *ATP11* overexpression plasmid were grown in HC-Ura
569 medium. All strains allowed to reach stationary phase (OD_{600} ~2.4) and subsequently shifted for
570 1 hr to medium lacking glucose. Samples were taken before and after dextrose depletion, iodine
571 (Sigma-Aldrich) was added to a final concentration of 0.5 mg/ml iodine. The intensities of
572 produced yellow-brown stain positively correlate with their intracellular glycogen levels.

573 **Accession Numbers**

574 The RNA-Seq data reported in this study is deposited in Gene Expression Omnibus (GEO)
575 database, and the accession number is GSE76444.

Acknowledgements

We thank C. Brown, M. Zavolan and J. Guimaraes for help with the data analysis and discussions, and M. Zavolan, I. G. Macara, T. Gross, R. P. Jansen and W. Filipowicz for critical comments on the manuscript. S. Ackerman and W. Olivas are acknowledged for providing the Atp11 antibody and the *PUF3* and *PUF5* constructs, respectively. This work was supported through grants from HFSP (RGP0031), the Swiss National Science Foundation (31003A_141207, 310030B_163480) and the University of Basel to AS. CW and JW were supported by Werner Siemens Fellowships and FS by SystemsX.ch (2009/025), the Swiss Initiative in Systems Biology.

Author Contributions

AS and CW conceived the project and experiments. Most experiments were performed by CW. JW was involved in initial experiments. FS, CW, NB and AS performed data analysis. AS, CW and FS wrote the manuscript with input from all authors.

Financial competing interests

The authors declare no competing financial interests.

Materials & Correspondence

Correspondence to: Anne Spang (anne.spang@unibas.ch).

Reference

Anders, S., Pyl, P.T., and Huber, W. (2015). HTSeq--a Python framework to work with high-throughput sequencing data. Bioinformatics 31, 166-169.

Anderson, J.S., and Parker, R.P. (1998). The 3' to 5' degradation of yeast mRNAs is a general mechanism for mRNA turnover that requires the SKI2 DEVH box protein and 3' to 5' exonucleases of the exosome complex. The EMBO journal 17, 1497-1506.

Andreassi, C., and Riccio, A. (2009). To localize or not to localize: mRNA fate is in 3'UTR ends. Trends in cell biology 19, 465-474.

Arribere, J.A., Doudna, J.A., and Gilbert, W.V. (2011). Reconsidering movement of eukaryotic mRNAs between polysomes and P bodies. Molecular cell 44, 745-758.

Ashe, M.P., De Long, S.K., and Sachs, A.B. (2000). Glucose depletion rapidly inhibits translation initiation in yeast. Molecular biology of the cell 11, 833-848.

Bailey, T.L., Boden, M., Buske, F.A., Frith, M., Grant, C.E., Clementi, L., Ren, J., Li, W.W., and Noble, W.S. (2009). MEME SUITE: tools for motif discovery and searching. Nucleic Acids Res 37, W202-208.

Balagopal, V., Fluch, L., and Nissan, T. (2012). Ways and means of eukaryotic mRNA decay. Biochimica et biophysica acta 1819, 593-603.

Bolger, A.M., Lohse, M., and Usadel, B. (2014). Trimmomatic: a flexible trimmer for Illumina sequence data. Bioinformatics 30, 2114-2120.

Brengues, M., Teixeira, D., and Parker, R. (2005). Movement of eukaryotic mRNAs between polysomes and cytoplasmic processing bodies. Science 310, 486-489.

Buchan, J.R., Muhlrad, D., and Parker, R. (2008). P bodies promote stress granule assembly in Saccharomyces cerevisiae. The Journal of cell biology 183, 441-455.

Buchan, J.R., Yoon, J.H., and Parker, R. (2011). Stress-specific composition, assembly and kinetics of stress granules in Saccharomyces cerevisiae. Journal of cell science 124, 228-239.

626 Cai, Y., and Futcher, B. (2013). Effects of the yeast RNA-binding protein Whi3 on the half-life
627 and abundance of CLN3 mRNA and other targets. PloS one 8, e84630.
628 Cao, L., Tang, Y., Quan, Z., Zhang, Z., Oliver, S.G., and Zhang, N. (2016). Chronological
629 Lifespan in Yeast Is Dependent on the Accumulation of Storage Carbohydrates Mediated by
630 Yak1, Mck1 and Rim15 Kinases. PLoS genetics 12, e1006458.
631 Chritton, J.J., and Wickens, M. (2010). Translational repression by PUF proteins in vitro. Rna
632 16, 1217-1225.
633 Chung, S., and Takizawa, P.A. (2011). In vivo visualization of RNA using the U1A-based tagged
634 RNA system. Methods Mol Biol 714, 221-235.
635 Davidson, A., Parton, R.M., Rabouille, C., Weil, T.T., and Davis, I. (2016). Localized Translation
636 of gurken/TGF-alpha mRNA during Axis Specification Is Controlled by Access to Orb/CPEB on
637 Processing Bodies. Cell reports 14, 2451-2462.
638 Decker, C.J., and Parker, R. (2012). P-bodies and stress granules: possible roles in the control
639 of translation and mRNA degradation. Cold Spring Harbor perspectives in biology 4, a012286.
640 Garcia, J.F., and Parker, R. (2015). MS2 coat proteins bound to yeast mRNAs block 5' to 3'
641 degradation and trap mRNA decay products: implications for the localization of mRNAs by MS2-
642 MCP system. Rna 21, 1393-1395.
643 Gauss, R., Trautwein, M., Sommer, T., and Spang, A. (2005). New modules for the repeated
644 internal and N-terminal epitope tagging of genes in Saccharomyces cerevisiae. Yeast 22, 1-12.
645 Gerber, A.P., Herschlag, D., and Brown, P.O. (2004). Extensive association of functionally and
646 cytotopically related mRNAs with Puf family RNA-binding proteins in yeast. PLoS biology 2,
647 E79.
648 Goldstrohm, A.C., Hook, B.A., Seay, D.J., and Wickens, M. (2006). PUF proteins bind Pop2p to
649 regulate messenger RNAs. Nat Struct Mol Biol 13, 533-539.
650 Hafner, M., Landthaler, M., Burger, L., Khorshid, M., Hausser, J., Berninger, P., Rothballer, A.,
651 Ascano, M., Jr., Jungkamp, A.C., Munschauer, M., et al. (2010). Transcriptome-wide

identification of RNA-binding protein and microRNA target sites by PAR-CLIP. Cell 141, 129-141.

Hey, F., Czyzewicz, N., Jones, P., and Sablitzky, F. (2012). DEF6, a novel substrate for the Tec kinase ITK, contains a glutamine-rich aggregation-prone region and forms cytoplasmic granules that co-localize with P-bodies. J Biol Chem 287, 31073-31084.

Hocine, S., Raymond, P., Zenklusen, D., Chao, J.A., and Singer, R.H. (2013). Single-molecule analysis of gene expression using two-color RNA labeling in live yeast. Nature methods 10, 119-121.

Huch, S., Gommlich, J., Muppavarapu, M., Beckham, C., and Nissan, T. (2016). Membrane-association of mRNA decapping factors is independent of stress in budding yeast. Scientific reports 6, 25477.

Janke, C., Magiera, M.M., Rathfelder, N., Taxis, C., Reber, S., Maekawa, H., Moreno-Borchart, A., Doenges, G., Schwob, E., Schiebel, E., et al. (2004). A versatile toolbox for PCR-based tagging of yeast genes: new fluorescent proteins, more markers and promoter substitution cassettes. Yeast 21, 947-962.

Kedersha, N., Stoecklin, G., Ayodele, M., Yacono, P., Lykke-Andersen, J., Fritzler, M.J., Scheuner, D., Kaufman, R.J., Golan, D.E., and Anderson, P. (2005). Stress granules and processing bodies are dynamically linked sites of mRNP remodeling. J Cell Biol 169, 871-884.

Kedersha, N.L., Gupta, M., Li, W., Miller, I., and Anderson, P. (1999). RNA-binding proteins TIA-1 and TIAR link the phosphorylation of eIF-2 alpha to the assembly of mammalian stress granules. The Journal of cell biology 147, 1431-1442.

Kilchert, C., Weidner, J., Prescianotto-Baschong, C., and Spang, A. (2010). Defects in the secretory pathway and high Ca2+ induce multiple P-bodies. Mol Biol Cell 21, 2624-2638.

Kishore, S., Jaskiewicz, L., Burger, L., Hausser, J., Khorshid, M., and Zavolan, M. (2011). A quantitative analysis of CLIP methods for identifying binding sites of RNA-binding proteins. Nature methods 8, 559-564.

678 Knop, M., Siegers, K., Pereira, G., Zachariae, W., Winsor, B., Nasmyth, K., and Schiebel, E.
679 (1999). Epitope tagging of yeast genes using a PCR-based strategy: more tags and improved
680 practical routines. Yeast 15, 963-972.
681 Kulkarni, M., Ozgur, S., and Stoecklin, G. (2010). On track with P-bodies. Biochemical Society
682 transactions 38, 242-251.
683 Langmead, B., Trapnell, C., Pop, M., and Salzberg, S.L. (2009). Ultrafast and memory-efficient
684 alignment of short DNA sequences to the human genome. Genome biology 10, R25.
685 Lavut, A., and Raveh, D. (2012). Sequestration of highly expressed mRNAs in cytoplasmic
686 granules, P-bodies, and stress granules enhances cell viability. PLoS genetics 8, e1002527.
687 Ling, Y.H., Wong, C.C., Li, K.W., Chan, K.M., Boukamp, P., and Liu, W.K. (2014). CCHCR1
688 interacts with EDC4, suggesting its localization in P-bodies. Exp Cell Res 327, 12-23.
689 Liu, J., Valencia-Sanchez, M.A., Hannon, G.J., and Parker, R. (2005). MicroRNA-dependent
690 localization of targeted mRNAs to mammalian P-bodies. Nature cell biology 7, 719-723.
691 Maeder, C.I., Hink, M.A., Kinkhabwala, A., Mayr, R., Bastiaens, P.I., and Knop, M. (2007).
692 Spatial regulation of Fus3 MAP kinase activity through a reaction-diffusion mechanism in yeast
693 pheromone signalling. Nature cell biology 9, 1319-1326.
694 Mager, W.H., and Ferreira, P.M. (1993). Stress response of yeast. The Biochemical journal 290
695 (Pt 1), 1-13.
696 Middleton, S.A., and Kim, J. (2014). NoFold: RNA structure clustering without folding or
697 alignment. Rna 20, 1671-1683.
698 Miller, C., Schwalb, B., Maier, K., Schulz, D., Dumcke, S., Zacher, B., Mayer, A., Sydow, J.,
699 Marcinowski, L., Dolken, L., et al. (2011). Dynamic transcriptome analysis measures rates of
700 mRNA synthesis and decay in yeast. Mol Syst Biol 7, 458.
701 Mitchell, S.F., Jain, S., She, M., and Parker, R. (2013). Global analysis of yeast mRNPs. Nature
702 structural & molecular biology 20, 127-133.

703 Munchel, S.E., Shultzaberger, R.K., Takizawa, N., and Weis, K. (2011). Dynamic profiling of
704 mRNA turnover reveals gene-specific and system-wide regulation of mRNA decay. Molecular
705 biology of the cell 22, 2787-2795.
706 Pelechano, V., Wei, W., and Steinmetz, L.M. (2015). Widespread Co-translational RNA Decay
707 Reveals Ribosome Dynamics. Cell 161, 1400-1412.
708 Quain, D.E., and Tubb, R.S. (1983). A Rapid and Simple Method for the Determination of
709 Glycogen in Yeast. J I Brewing 89, 38-40.
710 Ritz, A.M., Trautwein, M., Grassinger, F., and Spang, A. (2014). The prion-like domain in the
711 exomer-dependent cargo Pin2 serves as a trans-Golgi retention motif. Cell reports 7, 249-260.
712 Robinson, M.D., McCarthy, D.J., and Smyth, G.K. (2010). edgeR: a Bioconductor package for
713 differential expression analysis of digital gene expression data. Bioinformatics 26, 139-140.
714 Schmitt, M.E., Brown, T.A., and Trumpower, B.L. (1990). A rapid and simple method for
715 preparation of RNA from Saccharomyces cerevisiae. Nucleic acids research 18, 3091-3092.
716 Sen, G.L., and Blau, H.M. (2005). Argonaute 2/RISC resides in sites of mammalian mRNA
717 decay known as cytoplasmic bodies. Nature cell biology 7, 633-636.
718 Sherman, F. (1991). Getting started with yeast. Methods Enzymol 194, 3-21.
719 Sheth, U., and Parker, R. (2003). Decapping and decay of messenger RNA occur in
720 cytoplasmic processing bodies. Science 300, 805-808.
721 Souquere, S., Mollet, S., Kress, M., Dautry, F., Pierron, G., and Weil, D. (2009). Unravelling the
722 ultrastructure of stress granules and associated P-bodies in human cells. Journal of cell science
723 122, 3619-3626.
724 Stewart, M.S., Krause, S.A., McGhie, J., and Gray, J.V. (2007). Mpt5p, a stress tolerance- and
725 lifespan-promoting PUF protein in Saccharomyces cerevisiae, acts upstream of the cell wall
726 integrity pathway. Eukaryotic cell 6, 262-270.
727 Stoecklin, G., and Kedersha, N. (2013). Relationship of GW/P-bodies with stress granules.
728 Advances in experimental medicine and biology 768, 197-211.

729 Storici, F., and Resnick, M.A. (2006). The delitto perfetto approach to in vivo site-directed
730 mutagenesis and chromosome rearrangements with synthetic oligonucleotides in yeast.
731 Methods Enzymol 409, 329-345.
732 Stracka, D., Jozefczuk, S., Rudroff, F., Sauer, U., and Hall, M.N. (2014). Nitrogen source
733 activates TOR (target of rapamycin) complex 1 via glutamine and independently of Gtr/Rag
734 proteins. The Journal of biological chemistry 289, 25010-25020.
735 Sun, M., Schwalb, B., Pirkl, N., Maier, K.C., Schenk, A., Failmezger, H., Tresch, A., and
736 Cramer, P. (2013). Global analysis of eukaryotic mRNA degradation reveals Xrn1-dependent
737 buffering of transcript levels. Molecular cell 52, 52-62.
738 Sweet, T., Kovalak, C., and Coller, J. (2012). The DEAD-box protein Dhh1 promotes decapping
739 by slowing ribosome movement. PLoS biology 10, e1001342.
740 Tagwerker, C., Flick, K., Cui, M., Guerrero, C., Dou, Y., Auer, B., Baldi, P., Huang, L., and
741 Kaiser, P. (2006). A tandem affinity tag for two-step purification under fully denaturing
742 conditions: application in ubiquitin profiling and protein complex identification combined with in
743 vivocross-linking. Mol Cell Proteomics 5, 737-748.
744 Takizawa, P.A., Sil, A., Swedlow, J.R., Herskowitz, I., and Vale, R.D. (1997). Actin-dependent
745 localization of an RNA encoding a cell-fate determinant in yeast. Nature 389, 90-93.
746 Teixeira, D., Sheth, U., Valencia-Sanchez, M.A., Brengues, M., and Parker, R. (2005).
747 Processing bodies require RNA for assembly and contain nontranslating mRNAs. RNA 11, 371-
748 382.
749 Vuppalanchi, D., Coleman, J., Yoo, S., Merianda, T.T., Yadhati, A.G., Hossain, J., Blesch, A.,
750 Willis, D.E., and Twiss, J.L. (2010). Conserved 3'-untranslated region sequences direct
751 subcellular localization of chaperone protein mRNAs in neurons. The Journal of biological
752 chemistry 285, 18025-18038.

753 Weidner, J., Wang, C., Prescianotto-Baschong, C., Estrada, A.F., and Spang, A. (2014). The
754 polysome-associated proteins Scp160 and Bfr1 prevent P body formation under normal growth
755 conditions. J Cell Sci 127, 1992-2004.
756 Weil, T.T., Parton, R.M., Herpers, B., Soetaert, J., Veenendaal, T., Xanthakis, D., Dobbie, I.M.,
757 Halstead, J.M., Hayashi, R., Rabouille, C., et al. (2012). Drosophila patterning is established by
758 differential association of mRNAs with P bodies. Nat Cell Biol 14, 1305-1313.
759 Wickens, M., Bernstein, D.S., Kimble, J., and Parker, R. (2002). A PUF family portrait: 3'UTR
760 regulation as a way of life. Trends in genetics : TIG 18, 150-157.
761 Wilinski, D., Qiu, C., Lapointe, C.P., Nevil, M., Campbell, Z.T., Tanaka Hall, T.M., and Wickens,
762 M. (2015). RNA regulatory networks diversified through curvature of the PUF protein scaffold.
763 Nat Commun 6, 8213.
764 Wilson, W.A., Wang, Z., and Roach, P.J. (2002). Analysis of respiratory mutants reveals new
765 aspects of the control of glycogen accumulation by the cyclin-dependent protein kinase Pho85p.
766 FEBS letters 515, 104-108.
767 Wu, J., Zhang, N., Hayes, A., Panoutsopoulou, K., and Oliver, S.G. (2004). Global analysis of
768 nutrient control of gene expression in Saccharomyces cerevisiae during growth and starvation.
769 Proceedings of the National Academy of Sciences of the United States of America 101, 3148-
770 3153.
771 Zeiner, G.M., Cleary, M.D., Fouts, A.E., Meiring, C.D., Mocarski, E.S., and Boothroyd, J.C.
772 (2008). RNA analysis by biosynthetic tagging using 4-thiouracil and uracil
773 phosphoribosyltransferase. Methods in molecular biology 419, 135-146.
774 Zenklusen, D., Larson, D.R., and Singer, R.H. (2008). Single-RNA counting reveals alternative
775 modes of gene expression in yeast. Nat Struct Mol Biol 15, 1263-1271.
776 Zenklusen, D., Wells, A.L., Condeelis, J.S., and Singer, R.H. (2007). Imaging real-time gene
777 expression in living yeast. CSH Protoc 2007, pdb prot4870.

778